Photochemically Activated 3D Printing Inks: Current Status, Challenges, and Opportunities

Steven C. Gauci, Aleksandra Vranic, Eva Blasco, Stefan Bräse, Martin Wegener, Christopher Barner-Kowollik*

S. Gauci, C. Barner-Kowollik

School of Chemistry and Physics

Queensland University of Technology (QUT)

2 George Street, Brisbane, QLD 4000, Australia
E-mail: christopher.barnerkowollik@qut.edu.au

A. Vranic, S. Bräse

Institute of Organic Chemistry (IOC)

Karlsruhe institute of Technology (KIT)

Fritz-Haber-Weg 6, 76133 Karlsruhe, Germany

E. Blasco

Institute for Molecular Systems Engineering and Advanced Materials (IMSEAM)

Heidelberg University

Heidelberg 69120, Germany

S. Bräse

Institute of Biological and Chemical Systems-Functional Molecular Systems (IBCS-FMS)

Karlsruhe Institute of Technology (KIT)

76133 Karlsruhe, Germany

M. Wegener

Institute of Applied Physics (APH)

Karlsruhe Institute of Technology (KIT)

76128 Karlsruhe, Germany

E. Blasco, M. Wegener, C. Barner-Kowollik

Institute of Nanotechnology (INT)

Karlsruhe Institute of Technology (KIT)

76344 Eggenstein-Leopoldshafen, Germany

2

WILEY-VCH

Abstract: 3D printing with light is enabled by the photochemistry underpinning it. Without fine control over our ability to photochemically gate covalent bond formation by the light at a certain wavelength and intensity, advanced photoresists with functions spanning from on-demand degradability, adaptability, rapid printing speeds and tailored functionality are impossible to design. Herein, we critically assess recent advances in photoresist design for light-driven 3D printing applications and provide an outlook of the outstanding challenges and opportunities. We achieve this by classing the discussed photoresists in chemistries that function photoinitiator-free and those that require a photoinitiator to proceed. Such a taxonomy is based on the efficiency with which photons are able to generate covalent bonds, with each concept featuring distinct advantages and drawbacks.
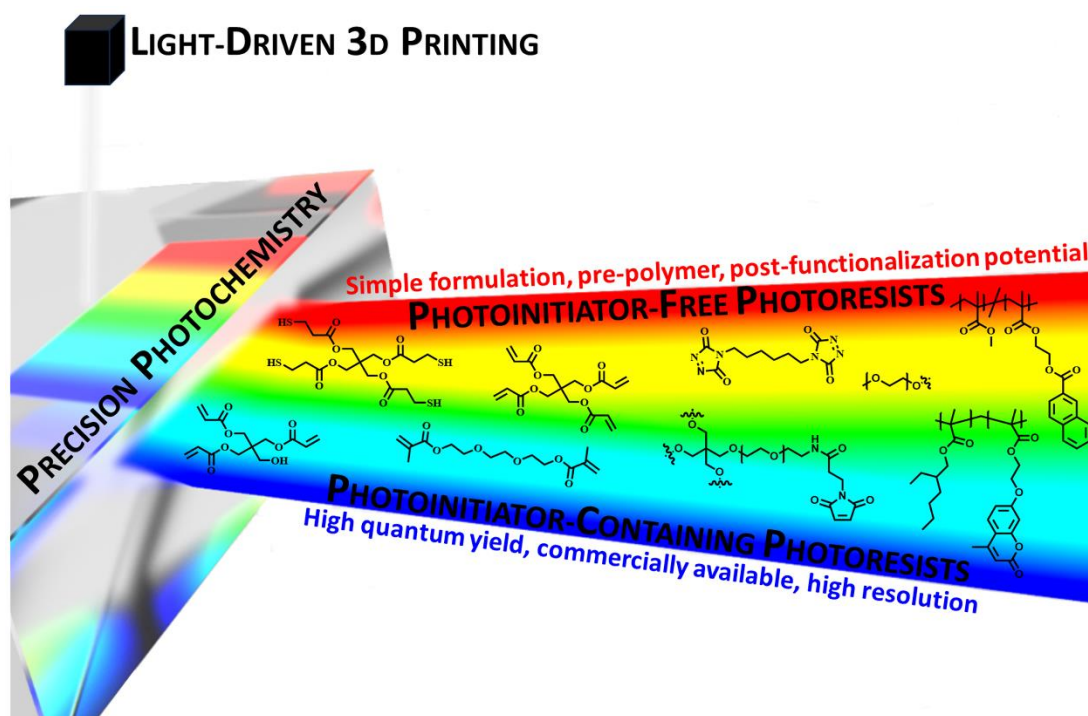
Figure 1. The taxonomy of the current review: photoresists for light-driven 3D printing that function photoinitiator-free and those that require a photoinitiator to proceed.

1. Introduction

Our world is transforming rapidly – from the rise of powerful artificial intelligence systems[1-3] to the on-going on-demand additive manufacturing drive.[4-8] These changes are underpinned by fundamental research efforts that question the way in which existing paradigms can be challenged, while pushing the limits of the currently possible. In light-driven 3D printing,[9,10] the engine room for a substantial part of the ongoing innovations is the photochemistry that governs the light-induced curing processes. Over the past years, we have explored in detail how light induces chemical reactions – via so-called photochemical action plots[11,12] – and found the unexpected: The UV/Vis absorbance spectrum of a photochemically reactive chromophore is no valid predictor of photochemical reactivity for all to-date investigated covalent bond forming reactions,[13-16] and some bond cleaving systems, too.[17] Specifically, we found that photochemical reactivity is substantially red-shifted compared to the absorption maximum of the UV/Vis spectrum, frequently into regions where absorption is extremely low. While an encompassing explanation for these surprising findings is yet to emerge, they have been replicated in other laboratories[18,19] and are critical for designing precision photocuring systems of the future. While photochemical action plots are highly relevant in predicting the behavior of photoresists that rely on single-photon absorption processes, such as stereolithography (SLA) and digital light processing (DLP), they may not fully reflect the complexity of a two-photon absorption (TPA) process as employed in 3D laser lithography. Recording two-photon action plots is an outstanding feat that is technically difficult to achieve – although it would critically assist designing photoresists for 3D laser lithography. The difficulties are associated with the only small irradiations volumes, making photochemical yield measurements challenging. Nevertheless, the contemporary design of photoresists is starting to be influenced by action plot data, as these provide essential insights into photochemically orthogonal, synergistic, and antagonistic reaction systems and the optimum wavelength of photochemical processes.[20-22] We refer the reader to our recent perspective on action plot technology and a precise definition of the taxonomy of precision photochemistry.[11]

In the current review, we focus on the latest developments in photochemical photoresist design for light-driven 3D printing applications, including 3D laser lithography,[23,24] SLA[25-28] and DLP,[29,30] with an emphasis on the last 5 years. Importantly, we wish to place the progress made to date into the context of a forward projection on what we believe is realistically possible to achieve in the next

decade based on the progress in our and the fields understanding of photochemistry. Thus, our current review initially introduces the key role precision photochemistry plays in 3D printing, followed by a brief discussion of the most widely employed light-driven 3D printing technologies. Subsequently, the focus will shift towards the reaction mechanisms of photoresists, highlighting recently developed photoresists that function photoinitiator-free, and those that require a photoinitiator to proceed. To conclude, the future trajectory and outstanding challenges of photoresist design are discussed.

2. Photochemistry in 3D Printing

Controlling chemical reactivity is the cornerstone of all key biological and chemical processes. Replicating these processes synthetically, however, has long been a formidable challenge and one that chemists have endeavored to overcome for decades.[31,32] To realize this goal, it is critical to apply external stimuli that can address reactivity selectively and without perturbing the overall system. One attractive option for achieving precise control over chemical transformations is the use of light.[33,34] Indeed, using light as an external stimulus to control chemical reactions is not a new concept. Giacomo Ciamician – considered one of the pioneers of photochemistry – envisaged using solar energy as a power source for human civilization in 1912.[35] Meanwhile, in 1958, the isomerization of Santonin to Lumisantonin represented one of the earliest examples of an organic transformation triggered by light.[36] Even today, the ability to use light as fuel to direct chemical synthesis precisely remains one of the most important and fascinating tools a chemist holds for several reasons. For example, light-triggered reactions are non-invasive, feature exceptional spatiotemporal and energy precision, and can be executed at ambient temperatures.[37] In addition, by appropriately adjusting the wavelength of light, it is possible to unlock an unparalleled level of control over chemical reactivity.[38]

In the context of 3D printing, the photochemistry involved in the light-induced curing process of a photoresist holds an indispensable role. If photochemistry was the painter, who uses different colors to create a masterpiece, then the photoresist assumes the role of the canvas, providing a foundation for the generation of intricate patterns and structures. Thus, photoresists are light-sensitive materials that can undergo a distinct transformation upon exposure to light of a specific wavelength. In general, photoresists can be separated into two groups, i.e., positive-tone and negative-tone resists (**Figure**

WILEY-VCH

2a).[39] For positive-tone, the photoresist is typically spin-coated onto a glass substrate. Thus, the desired thickness of the photoresist is controlled by the spinning speed and the time for pre-exposure baking, which occurs immediately after the spinning. Subsequently, the solid photoresist is selectively – through a photomask[40] or direct printing methods[41] – exposed to light. Consequently, the exposed area of the photoresist becomes soluble and can be washed away in a subsequent developing step, leaving behind the unexposed region (**Figure 2a**). The advantages of using positive-tone resists include ease of preparation and processing, high pattern and/or feature resolution, and compatibility with a wide range of substrates. Thus, these photoresists have been used in various fields, such as semiconductor manufacturing,[42] microelectronics,[43] and optical device fabrication.[44,45] In contrast to positive-tone, negative-tone photoresists behave in the opposite manner. Specifically, the area exposed by light is crosslinked and an insoluble network is formed. Accordingly, the crosslinked region remains on the substrate, while the unexposed region is removed in a developing step (**Figure 2a**). Negative-tone resists provide versatility in terms of exposure conditions, enabling their use in a wide range of additive manufacturing techniques,[46-48] thereby expanding the possibilities of fabricating complex 3D structures with high precision. In addition, they often require fewer processing steps compared to positive-tone resists, thus saving time, and reducing costs. As a result, negative-tone photoresists have found utility in various applications including prototyping,[49] medicine,[50,51] as well as everyday situations such as households and schools.[52]

Since Niepce's pioneering work in 1826, which marked the generation of the first lithographic image, photoresist technology has made significant advances.[53-55] Such advances have paved the way for the generation of materials that are stimulus-responsive[56-60] and have unlocked exciting possibilities in meta-material designs that verge on the realm of science-fiction, such as the intriguing concept of invisibility cloaks.[61] Nevertheless, there are several fascinating properties that still elude current photoresist technology. For example, photoresists that are mechanically compliant and possess the ability to repair themselves autonomously or programmatically when damaged. In addition, photoresists that can be printed with wavelengths exceeding 1000 nm, and those that can be erased specifically by green – or even longer –wavelengths. Another example – which is only emerging – is wavelength-orthogonal printing, enabling the incorporation of multiple properties into a single printed structure from one resist cartridge.[62] While these examples are currently – at least partly –

hypothetical, continued in-depth understanding of photoresists will lead to breakthroughs that push the boundaries of what photoresists can accomplish.
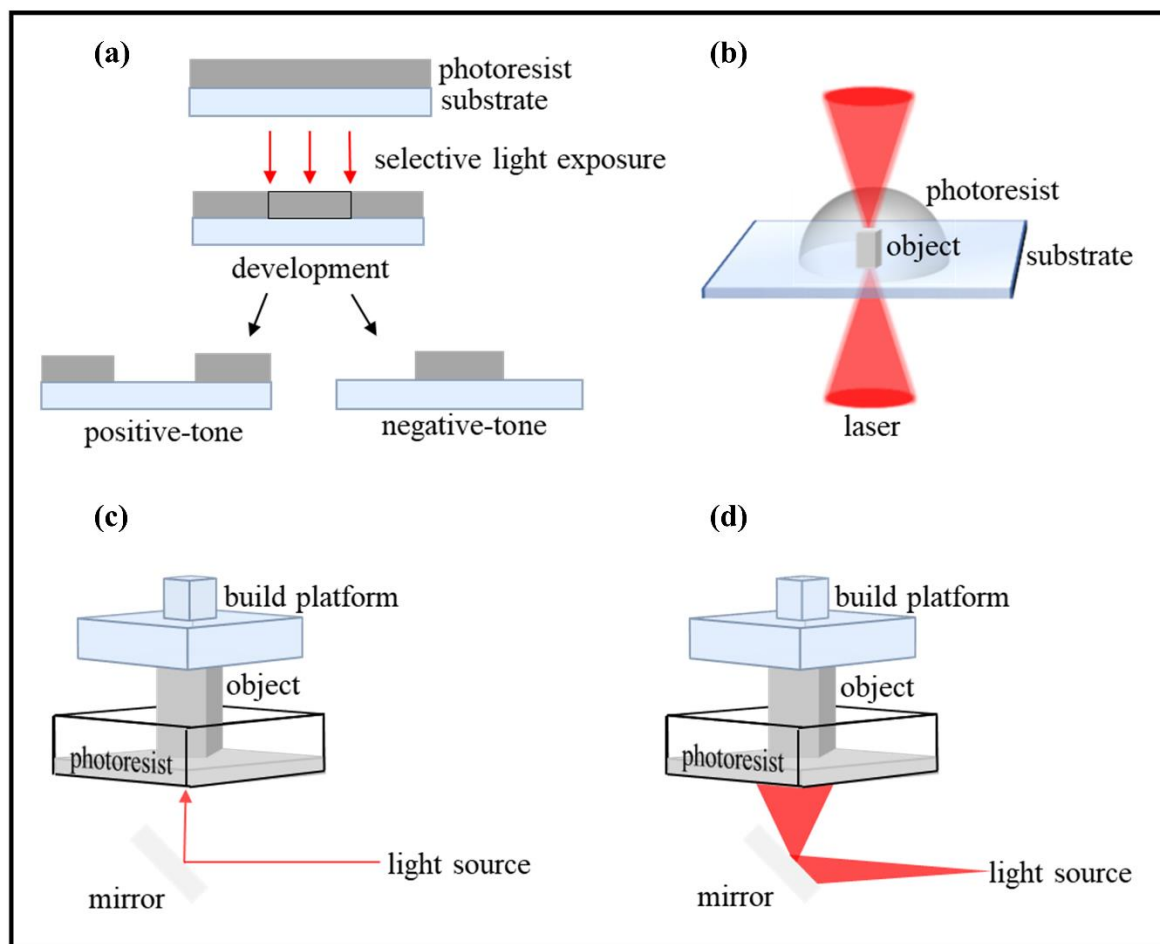
Figure 2. (a) Schematic representation of the two distinct photoresists, i.e., positive-tone and negative-tone resists. (b-d) Light-driven 3D printing techniques: (b) direct laser writing, (c) stereolithography and (d) digital light processing.

3. Light-Driven 3D Printing Techniques

Before discussing photoresist mechanisms (**Section 4**), the main light-driven 3D printing techniques, i.e., 3D laser lithography, stereolithography and digital light processing, will be briefly discussed.

3.1. 3D Laser Lithography

3D Laser Lithography – also known as direct laser writing (DLW) – has become one of the most versatile and routinely used techniques for fabricating 3D printed structures on the microscopic scale.[63] DLW exploits the optical phenomenon of two-photon absorption (TPA), in which a femtosecond – pulsed – laser is tightly focused into the volume of a photoresist, which is on a transparent substrate (**Figure 2b**). Consequently, this phenomenon is constrained to a very small volume element called a 'voxel', and accumulation effects in the periphery are suppressed, thus enabling the fabrication of near-arbitrary 3D structures with sub-100 nm scale resolution.[63,64] Accordingly, DLW has been utilized to fabricate a plethora of highly resolved structures that find use in a large variety of applications, including cell biology,[65,66] photonics,[67,68] and microneedle devices.[69]

3.2. Stereolithography

Stereolithography (SLA) was pioneered by Hull *et al*. in 1986[70] and is known to be one of the first experimentally realized light-driven 3D printing techniques. In general, an SLA system consists of a light source, a liquid photoresist vat and a build platform (**Figure 2c**). During the process of SLA printing, the photoresist undergoes a liquid-to-solid transformation upon point-by-point exposure to light. This transformation occurs within seconds, enabling the gradual construction of the 3D-printed structure in a layer-by-layer fashion. The successful execution of SLA printing relies on two key parameters: the speed of photocuring and the viscosity of the resin.[71] Rapid photocuring ensures that each layer of the object solidifies quickly, while low resin viscosity allows for swift resin flow across the build platform, facilitating the formation of new layers.

3.3. Digital Light Processing

In digital light processing (DLP), a light source irradiates the liquid photoresist, and an entire layer can be cured all-at-once instead of point-by-point curing in SLA (**Figure 2d**). Consequently, DLP allows

WILEY-VCH

faster printing speeds than SLA while still maintaining high fabrication accuracy. Thus far, DLP has been utilized to print a wide variety of structures that have been used for tissue engineering[72-74] and for drug delivery systems.[75,76] In 2015, DeSimone and co-workers reported a variation of DLP called continuous liquid interface printing (CLIP).[77] In CLIP, an oxygen-permeable window is employed to create a 'dead zone' at the bottom of the photoresist vat, thereby inhibiting free-radical polymerization. Consequently, this oxygen-inhibited dead zone enables fast printing speeds and layer-less part construction.

4. Photoresist Mechanisms in 3D Printing

A variety of photoinduced reactions can be performed within the excitation volume of a photoresist. These reactions play a key role in governing the chemical properties of the photoresist, which ultimately influence the photosensitivity (i.e., quantum yield) and functionality of the resist in 3D printing applications. According to the photochemical equivalence law, every reacting molecule will absorb one quantum of energy. However, there are many reactions where the 1:1 correlation between the number of quanta absorbed and the number of reacting molecules is not observed. Thus, the term quantum yield is used to explain this deviation in many photochemical reactions. In a photochemical reaction, two distinct processes are involved, i.e., primary, and secondary. In a primary process – a molecule after absorbing one quantum of radiation – is in an excited state with multiple pathways for energy dissipation, including the possibility for a subsequent chemical reaction. Thus, it is possible for the activated molecule to undergo secondary processes after absorbing only a single quantum of light. However, the number of chemical bonds formed in secondary processes can vastly differ, depending on the type of reaction. In the context of this review, the overall quantum yield can be defined as the number of bonds formed as a result of the absorption event and can vary widely from system to system. For example, the quantum yield of a cycloaddition will typically be well below unity in the vast majority of cases, even well below 0.1.[78] In contrast, photochemically induced chain-growth reactions exhibit much higher quantum yields – often approaching or exceeding 1.0 – due to the fact that one generated propagating radical center will lead to the formation of a large number of covalent bonds.[79] Thus, the taxonomy of the current review will be governed by the quantum yield
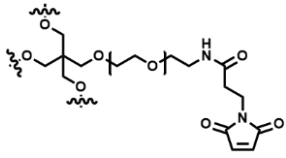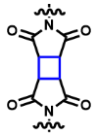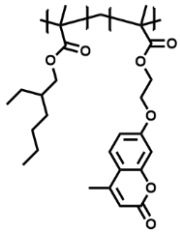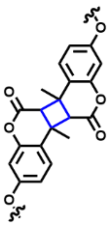
WILEY-VCH
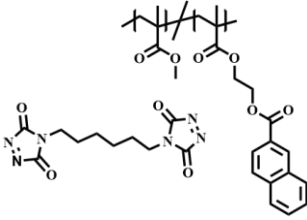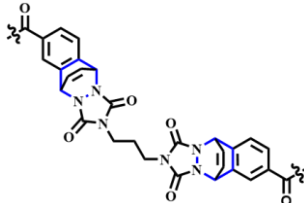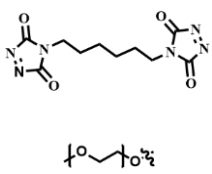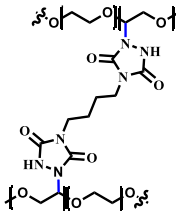
of the photochemical processes that govern the resists. Photoresists with high quantum yields are typically underpinned by free-radical chain-growth reactions containing a radical photoinitiator, while resists that rely on one or less bond formations per successful absorption event typically rely on non-chain-growth processes. As these two resist systems require substantially different printing parameters and have specific advantages and disadvantages, we will discuss the progress in photoresist chemistry using categories of 'Photoinitiator-Free' and 'Photoinitiator-Containing Photoresists' (**Section 4.1** and **4.2**, respectively). Notably, **Section 4.2** will exclusively cover free-radical processes since other polymerization methods, such as cationic polymerization warrant a separate review.

4.1. Photoinitiator-Free Photoresists

Photoinitiator-free photoresists do not rely on traditional photoinitiators to initiate polymerization or crosslinking reactions. They employ non-chain growth mechanisms to initiate the desired chemical transformation when exposed to light. The exclusion of photoinitiators in these photoresists offers several advantages, including simplified photoresist formulation and handling, reduced costs, pre-fabrication of polymer chains that are subsequently photochemically crosslinked and localized control over the crosslinking/polymerization process without diffusion of growing macromolecules into non-illuminated areas. However, a significant disadvantage of photoinitiator-free photoresists is their decreased photosensitivity, thus requiring a high exposure dose, resulting in slow writing speeds. As a result, a trade-off is always required when developing a photoresist to fabricate 3D structures. Within the current subsection, we will discuss examples of photoresists employing non-chain-growth mechanisms that have emerged in the last five years, highlighting important aspects such as the performance and function of the resist. **Table 1** collates the photoresists discussed in the current subsection, providing details regarding their composition, reaction conditions, and reaction mechanism of each photoresist. For additional examples of photoinitiator-free photoresist that have been utilized in 3D laser lithography, which are not discussed in this subsection, we refer the reader to other publications.[80-82]

Table 1. Photoinitiator-free photoresists for the purpose of light-driven 3D printing discussed in this subsection.

	Photoresist Composition	Reaction λ	Photoproduct	Ref
(a)		TPA 800 nm		90
(b)		365 nm		91
(c)		TPA 780 nm		104, 105
(d)		TPA 700 nm		106

Abbreviations: λ, Wavelength; TPA, Two-Photon Absorption; Ref, Reference

4.1.1. Photoaddition-Based Photoresists

Photoaddition reactions such as [2+2] and [4+4] photocycloadditions are considered thermally forbidden processes due to the geometric constraints on the frontier molecular orbitals of the participating π-bonds, which prevent the necessary overlap. Consequently, the concerted mechanism is only observed under photochemical conditions according to the Woodward-Hoffmann rules.[83]

Thus, when a conjugated alkene system is excited by a photon, the electron transitions to the π^* orbital, resolving the geometric constraints hindering the thermal reaction. Although photocycloadditions constitute one of the most frequently used reactions for chemical transformations,[84-89] their application in 3D printing has so far been limited. As noted above, the quantum yield of photocycloadditions is much lower compared to other radical polymerization mechanisms typically employed in light-driven 3D printing. Consequently, this fact limits the printing speed and efficiency, which makes them less practical for high-throughput 3D printing processes. Nevertheless, cycloadditions provide an extensive range of functional groups that can be incorporated into pre-formed polymer chains, rendering them compatible with existing 3D printing techniques. Another advantage includes the ability to modify the printed structure through post-functionalization or additional crosslinking on the basis of remaining functional units, thereby altering the chemical or mechanical properties of the structure post-printing with relative ease.

Werner and co-workers reported the photodimerization of maleimides under two-photon absorption conditions to fabricate hydrogel structures.[90] Here, the photoresist consisting of a four-armed maleimide-terminated polyethylene glycol – capable of undergoing [2+2] cycloaddition – was subjected to laser irradiation with various intensities and a constant writing speed of 15 um s^{-1} (**Table 1a**). Notably, the fabrication of well-defined hydrogel structures was only possible when the photoresist was irradiated with an 800 nm laser and when the intensity was increased from 40 to 80 mW (**Figure 3a**). Nevertheless, the hydrogel structures were fabricated without using a photoinitiator, thereby eliminating the difficulties related to photoinitiator solubility and cytotoxicity.

More recently, Benkhaled *et al*. demonstrated [2+2] photocycloaddition in DLP by employing a photoresist consisting of coumarin-based polymers P(EHMA$_x$-*co*-CoumMA$_y$) (**Table 1b** and **Figure 3b**).[91] Initially, the photoresist's suitability for DLP was investigated by irradiating P(EHMA$_x$-*co*-CoumMA$_y$) films with UV light (λ = 365 nm). The resulting crosslinked films show no signs of warping during irradiation. Meanwhile, differential scanning calorimetry measurements of the crosslinked films reveal that the glass transition temperature (T_g) of the material is dependent on the ratio of coumarin within the polymer, i.e., the T_g increases from 21 °C for P(EHMA$_{80}$-*co*-CoumMA$_{20}$), to 39 °C for P(EHMA$_{20}$-*co*-CoumMA$_{80}$). The coumarin-based photoresist was further utilized to fabricate a 3D butterfly structure with shape memory properties via DLP. Initially, the butterfly was fabricated with

open wings, which were closed and fixed in place by applying a temperature below the printed materials T_g. Subsequently, a progressive opening of the wings over 13 s was observed by applying a constant temperature above the materials T_g (**Figure 3c**). Interestingly, the authors do not mention the possibility of using other stimuli, such as, e.g., light, to induce movement and/or degradation, since coumarin dimers can be photochemically reversed.[92-94]
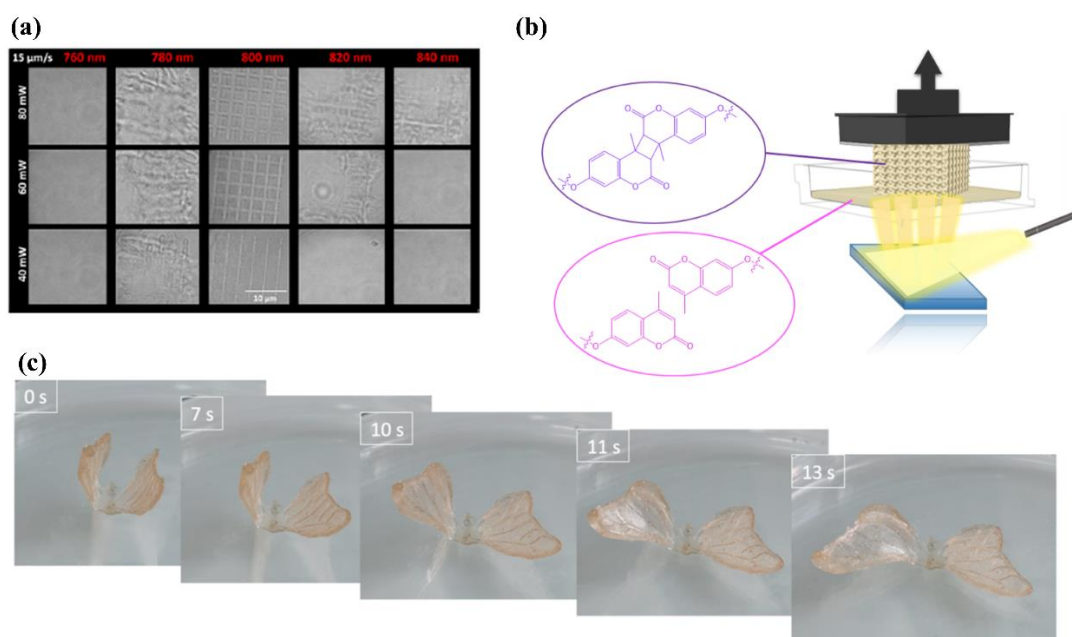
Figure 3. (a) Fabrication of hydrogels under different wavelengths and laser intensity at a writing speed of 15 μm s^{-1}. Adapted with permission.[90] Copyright 2017, American Chemical Society. (b) Illustration of the printing process via DLP, whereby irradiation with UV light induces the [2+2] cycloaddition of coumarin, and (c) 3D printed butterfly with shape memory properties, whereby the wings of the butterfly open after 13 s by applying a temperature above the printed materials Tg. Adapted with permission.[91] Copyright 2022, Elsevier.

One key advantage of utilizing a photocycloaddition mechanism for 3D printing applications is that – in some cases – the photocycloaddition products can be photochemically reversed. Specifically, one wavelength of light can be used for the printing process, while another wavelength of light can be used to erase the structure. Almost all photo-reversible cycloadditions occur via a [2+2] and [4+4] dimerization mechanism. Some of the compounds capable of undergoing [2+2] photo-reversible

dimerization include cinnamates, coumarin, and thymine.[95-97] Meanwhile, anthracene is a commonly used moiety capable of undergoing [4+4] photo-reversible dimerization.[98] However, one of the major disadvantages of these photo-reversible dimerization reactions is the inherent blue-shifted absorption of the cycloaddition product. Consequently, the high-energy UV light required to initiate cyclo-reversion can cause side reactions and be problematic for some applications.[32,99]

The ability to erase a 3D-printed structure post-printing and on-demand is currently another active field of research. Post-printing erasing is a highly enabling feature for the cleavage of valves and bridges in microfluidic devices, for the degradation of cellular scaffolds to trigger cell release, and for the removal of support materials after printing complex architectures. Such erasable parts often require harsh removal techniques, which can physically damage the printed structure and/or limit its application. In contrast, if the same 3D structure is constructed from a photoresist containing labile bonds and linkages, the redundant structures can be selectively erased by mild triggers.[24,100-103] Gauci *et al*. recently reported a photoresist for direct laser writing that is capable of fabricating microstructures that can be erased by the mildest trigger of all: darkness.[104,105] The photoresist is comprised of 1,6-hexamethylene bistriazolinedione (BisTAD) and a naphthalene-containing polymer (**Table 1c**). The chemistry that underpins this photoresist is the of-out-equilibrium photocycloaddition reaction between triazolinedione (TAD) and naphthalene that is, and remains, far shifted to the adduct side during irradiation. The formed adducts remain stable when continuously irradiated, but spontaneously dissociate when subjected to darkness. Thus, 3D microstructures were fabricated by exploiting the TAD/naphthalene photocycloaddition upon exposure to a 780 nm laser. Critically, the resulting micro-stars were shown to remain stable when continuously irradiated with a green light-emitting diode (**Figure 4a**, top right micro-star) yet degrade when exposed to darkness (**Figure 4a**, top left micro-star). In addition, the TAD-naphthalene photoresist was combined with a non-degradable resist to fabricate 3D multi-material scaffold-type structures (**Figure 4a**, bottom, left scaffold). Here, only the parts of the scaffold that was printed with the TAD-naphthalene photoresist (i.e., the connecting bridges) degraded after 9 days in the dark (**Figure 4a**, bottom, right scaffold).[104] In a following study, we further advanced the TAD-naphthalene photoresist by demonstrating the first instance where 3D structures consisting of both degradable and non-degradable segments are printed from a single photoresist.[105] Specifically, switching the laser intensity from 8.6 to 6.5 mW during the

fabrication process enabled the fabrication of 3D multi-functional structures from a single photoresist, whereby only the segments printed with 6.5 mW are degradable (**Figure 4b**). The strategy employed in the above example significantly simplifies the fabrication of multi-functional structures, which would otherwise require a separate photoresist to manufacture.

The BisTAD crosslinker was further exploited to fabricate 3D structures by Houck *et al*. (**Table 1d**).[106] Here, however, the photoresist is driven by the photoinduced TAD-ether conjugation. Specifically, upon UV or visible light irradiation, the TAD substrate readily undergoes an α-addition with ethers via a hydrogen extraction process. The resulting adducts contain hemiaminal-type linkages that can be hydrolyzed in an aqueous medium. Thus, 3D microstructures were fabricated via DLW by subjecting polyethylene glycol (PEG) and the BisTAD crosslinker to a 700 nm laser with varying laser intensity. The resulting boxing ring structures were immersed in deionized water at 37 °C, and their subsequent degradation over 36 h was monitored by time-lapse optical microscopy (**Figure 4c**). Notably, the TAD-PEG photoresist allowed for the fabrication of microstructures at a writing speed of 100 um s^{-1}, exhibiting a 10-fold acceleration compared to the TAD-naphthalene photoresist. Such an increase in printing speed could potentially expand the application of this photoresist to other 3D printing methods such as SLA or DLP, enabling the fabrication of larger-scale 3D structures.
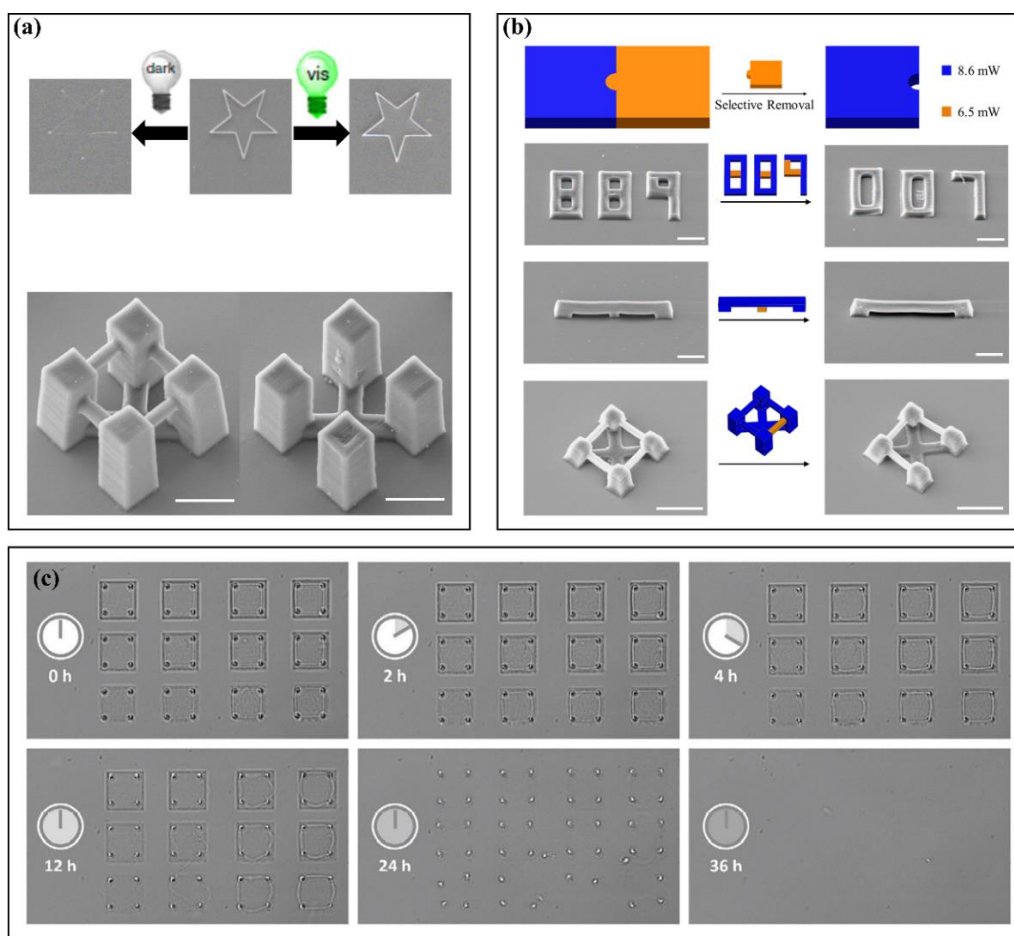
Figure 4. (a) SEM images of micro-stars printed from the TAD-naphthalene-based photoresist, which remain stable when continuously irradiated with green-light (right) yet degrade when exposed to darkness (left) and SEM images of multi-material scaffold-type structures whereby only the connecting bridges are erasable. Scale bars: 10 μm. Adapted with permission,[104] Copyright 2022, Wiley-VCH. (b) SEM images of multi-material structures printed exclusively from the TAD-naphthalene based photoresist, whereby only the parts printed with 6.5 mW are erasable when exposed to darkness. Scale bars: 10 μm. Adapted with permission,[105] Copyright-VCH. (c) Time-lapse optical microscopic imaging of the boxing-ring structures printed from the TAD-PEG photoresist being erased upon immersion in water at 37 °C. Adapted with permission,[106] Copyright 2022, Wiley-VCH.

WILEY-VCH

4.2. Photoinitiator-Containing Photoresists

Photoinitiator-containing photoresists typically comprise a multi-functional monomer as the basis of the crosslinked polymeric material and a photoinitiator that initiates the free radical-forming mechanism. In radical systems, the main steps include initiation, propagation, and termination. In 3D printing, the initiation steps occur when the photoinitiator absorbs light of a specific wavelength to generate the radical species. In general, photoinitiators can be separated into two categories, i.e., Norrish Type-I and Type-II. Whereas the former undergoes bond cleavage at the α-carbon to generate radical species, the radical species for Type-II photoinitiators are formed via a hydrogen abstraction mechanism involving a co-initiator.[107,108] Once the initiator-derived primary radicals are formed, they can react with the (multi-functional) monomers within the photoresist, involving an attack of the radical on the unsaturated bonds in the monomers, resulting in macromolecular chain growth. Concomitantly, radical-chain termination involves the removal of active radicals from the photoresist, which occurs through various processes including termination by recombination and disproportionation. For a more comprehensive discussion on photoinitiators, we refer the reader to recent publications.[9,109-111] In the current subsection, we will discuss recently developed photoresists based on chain-growth mechanisms. Specifically, we will discuss meth(acrylate)-based photoresists (**section 4.2.1**) and thiol-ene-based photoresists (**section 4.2.2**), highlighting their advantages, challenges, and functional aspects in 3D printing applications. The photoresists discussed in this subsection are compiled in **Table 2**, which collates details regarding the composition and reaction conditions of each photoresist.

Table 2. Photoinitiator-containing photoresists discussed in the current subsection.

Photoresist Composition		Reaction λ	Ref
Photoinitiator	Monomer		
(a)		TPA 780 nm	122
(b)		TSA 405 nm	125
(c)		TSA 405 & 640 nm	125
(d)		TPA 244 nm	126
(e)		TPA 200-300 nm	127
(f)		385 nm	134
(g)		385 nm	135

18

WILEY-VCH

(h)			TPA	149
			780 nm	
(i)	-		266 nm	150
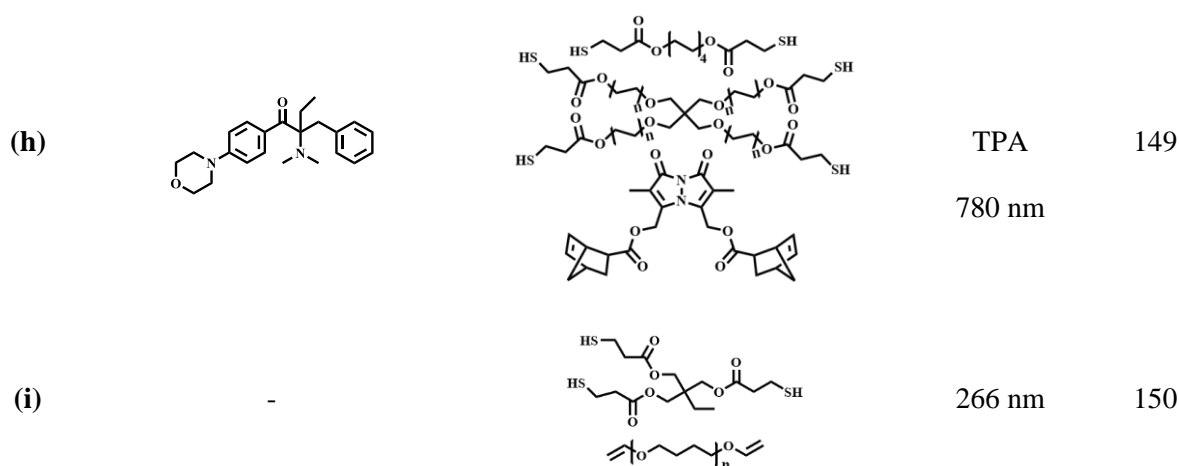
Abbreviations: λ, Wavelength; TPA, Two-Photon Absorption; TSA, Two-Step Absorption; Ref, Reference

4.2.1. (Meth)acrylate-Based Photoresists

(Meth)acrylate monomers such as – or derivatives thereof – triethylene glycol di(meth)acrylate (TEGMA / PEGDA),[112-114] trimethylolpropane triacrylate (TMPTA)[115,116] and pentaerythritol tri- or tetra-acrylate (PETA and PETTA)[100,117-120] are commonly used owing to their commercial availability and relatively large propagation-rate coefficients (**Figure 5**).[121] In addition, these monomers are viscous liquids, enabling them to dissolve small quantities of photoinitiator, which simplifies the formulation of the photoresist. Furthermore, the resulting polymeric material usually exhibits desirable properties, including resistance to elevated temperatures and inertness toward a wide range of solvents and additives. However, these properties are associated with a trade-off, and additional functionalization of the monomer unit is often required to fabricate structures that can respond and adapt to external stimuli after the printing process.
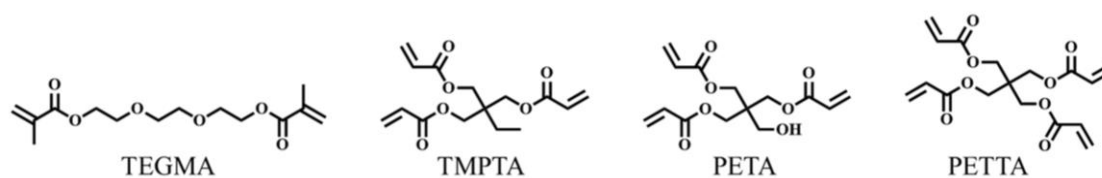
Figure 5. Examples of (meth)acrylate monomers commonly utilized in 3D printing.

19

Recently, Mattoli and co-workers developed a photoresist that allows the 3D printing of degradable microstructures via DLW.[122] The photoresist formulation consisted of a cyclic ketene acetal compound (MDO) in combination with (tetra-, tri-, and di-functional) acrylate crosslinkers and 5 wt% Omnirad 379 as photoinitiator (**Table 2a**). When the photoresist is subjected to a 780 nm laser, MDO undergoes radical ring-opening polymerization to form the corresponding aliphatic polyester moiety, which is subsequently incorporated into the crosslinking network. The addition of the labile ester moiety enables de-crosslinking on-demand upon treatment with suitable nucleophiles. The performance of the photoresist was demonstrated by fabricating solid and woodpile microstructures at a writing speed of 7500 and 2000 um s^{-1}, respectively (**Figure 6a-b**). After conducting several degradation tests, the authors found that immersing the microstructures, fabricated from a photoresist formulation consisting of 90% MDO and 10% PETA, into a methanol solution containing KOH (0.5 M) at 50 °C provided an ideal degradation environment. Finally, the MDO:PETA photoresist was combined with a non-degradable commercial resist to fabricate micro-donuts, whereby only the MDO:PETA printed segment degrades (**Figure 6c-d**).

WILEY-VCH
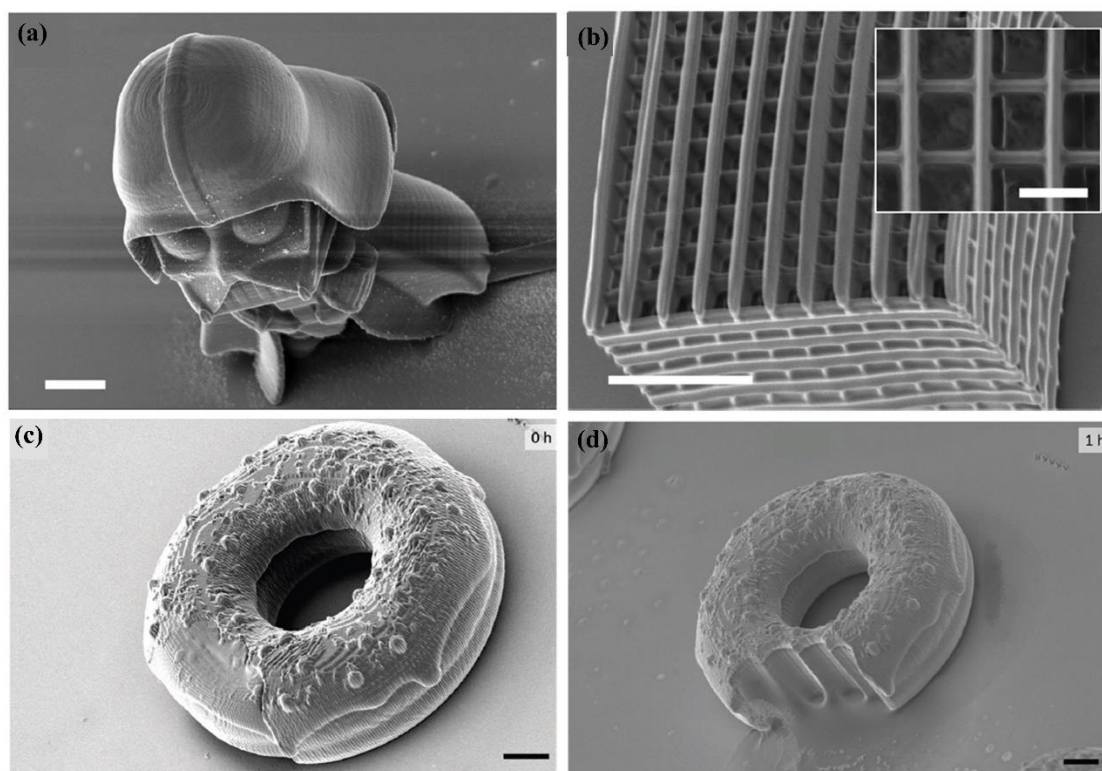
Figure 6. SEM images of microstructures fabricated via DLW. (a) A micro-Darth Vader, and (b) a woodpile structure. (c) A micro-donut printed with the MDO:PETA and non-degradable photoresists and (d) partial degradation of the micro-donut, whereby only the MDO:PETA printed segment degrades after 1 h. Scale bars: 20 µm, inset scale bar: 5 µm. Adapted with permission.[122] Copyright 2022, Wiley-VCH.

1,2-Diketones, especially benzil derivatives, have successfully been used as photoinitiators in combination with PETA for 3D laser nanoprinting by the Wegener group.[48] These authors suggested an avenue for radical formation of benzil-based photoinitiators, referred to as two-step absorption (TSA), illustrated in **Figure 7a**. The motivation behind two-step absorption is to replace the virtual intermediate state of TPA with a real excited state that exists in the absence of the light field. The lifetime of this electronic state is determined by non-radiative processes and can be a few picoseconds long. The electron population of the photoinitiator in the second excited state leads to its decomposition into radical species that initiate local crosslinking/polymerization of the liquid monomer, resulting in solidification in a small-volume element called a voxel.[123] TSA has been reported as a single-color absorption process as well as a two-color absorption process, with blue (405

WILEY-VCH

nm) and red (640 nm) light. Since benzil is a Norrish Type-I photoinitiator (**Figure 7b**), scavengers such as 2,2,6,6-tetramethylpiperidinyloxyl (TEMPO) are added to the resist in order to prevent side reactions like hydrogen abstraction by reducing the lifetime of the intermediate state T_1. It is assumed that the C-C bond in the benzil molecule is cleaved, giving rise to two identical radicals, which subsequently add to the monomer, generating a new radical which in turn adds to a monomer and thus continues the polymerization (**Figure 7c**).[10] After comprehensive publications on the three-dimensional printability of benzil and biacetyl,[124] the Wegener and Bräse groups explored alternative TSA photoinitiators for 3D laser nanoprinting.[125] 22 possible photoinitiator systems were evaluated, including asymmetrical diketones, heterocyclic rings and benzil derivatives with diverse substituents, e.g., halides, nitro- or methyl groups in varying steric positions. The composition of every photoresist included 100 mM of photoinitiator, and 50 mM of TEMPO dissolved in PETA. On the one hand, some molecules were excluded as photoinitiators due to their insolubility in acrylic monomers or the absence of reactivity at 405 nm. On the other hand, several diketones are suitable for 3D laser nanoprinting through two-step-absorption yet mostly only with blue light, a selection is shown in **Table 2b**. 1-Phenylpropane-1,2-dione, a structural combination of benzil and biacetyl, as well as 4,4-difluorobenzil and bisbenzil, have been proven to be potential initiator molecules for two-step-two-color-absorption processes with blue and red light (**Table 2c**). 3D structures printed with 3,3,5,5-tetramethylcyclopentane-1,2-dione are illustrated in **Figure 8**.
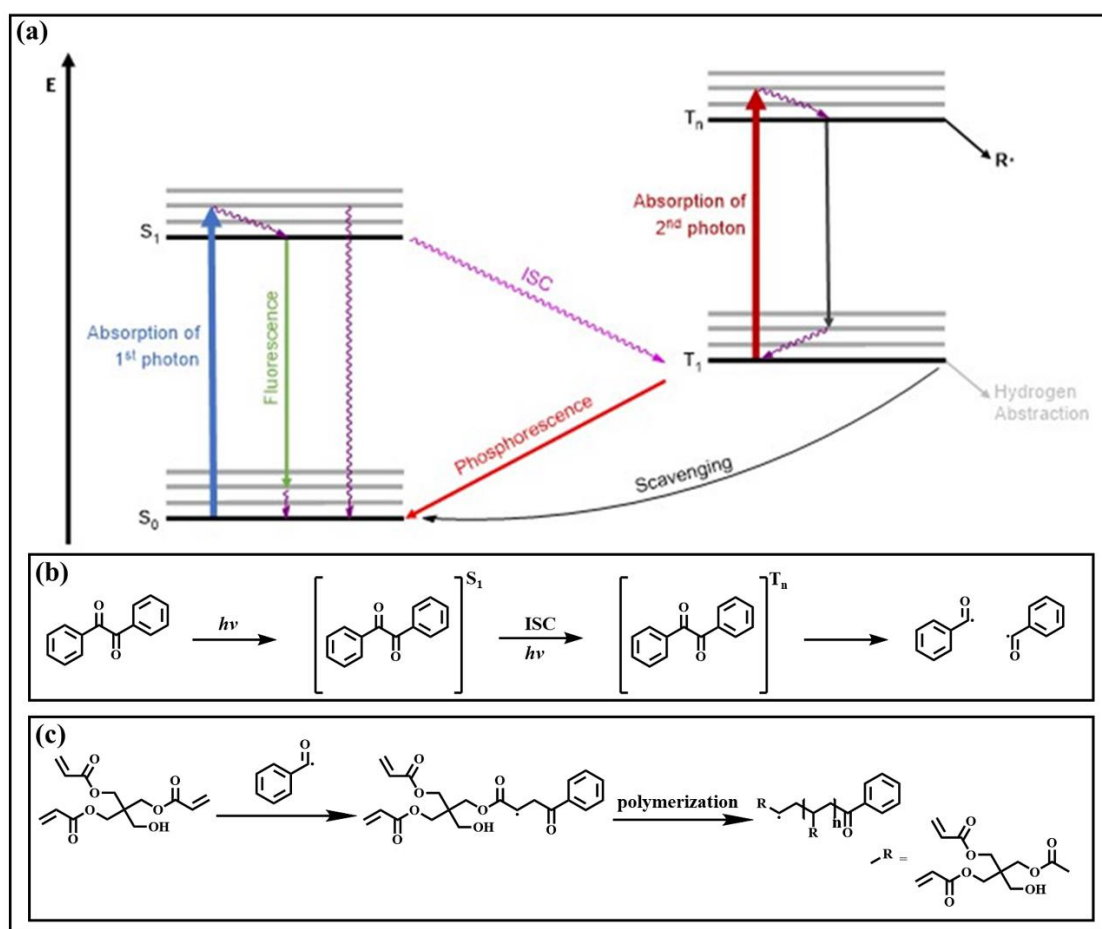
Figure 7. (a) Mechanism of two-step absorption: initially a photon is absorbed, leading to excitation of the initiator molecule from the ground state S_0 to the excited state S_1, from which the molecule can emit light in the form of fluorescence or transitions to the triplet state T_1 via intersystem crossing (ISC). Therefrom, the photon can be emitted in the form of phosphorescence, form a radical by hydrogen abstraction, or ideally absorb a second photon to a higher excited state T_n wherefrom the radical is generated.[48] (b) Norrish Type-I reaction on the example of benzil: by irradiation with light, the electrons are excited into the excited singlet state S_1, from which a transition into the triplet state T_1 can take place through ISC. Since benzil is a symmetrical molecule, the two radicals formed are identical.[107] (c) Radical photopolymerization of PETA initiated with a benzil-radical.[10]

23
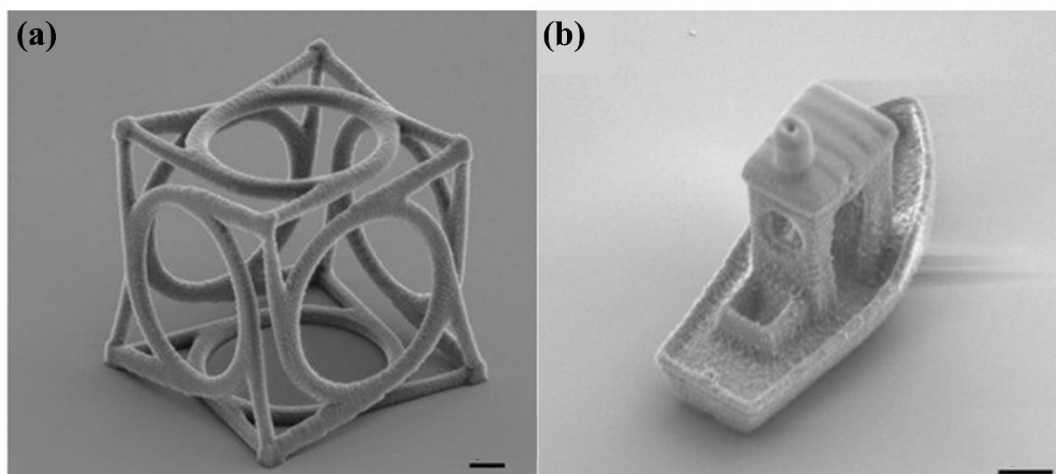
Figure 8. SEM images of microstructures printed with a 405 nm laser via two-step absorption. (a) Chiral metamaterial, at a power of P_{405} = 1.86 mW and a velocity of v = 500 μm s^{-1}. (b) #3DBenchy structure at P_{405} = 2.7 mW and a velocity of v = 1 mm s^{-1}. Scale bars: 2 μm. Adapted with permission.[125] Copyright 2022, Wiley-VCH.

In addition to 3D printing, Blasco and co-workers have used acrylate-based photoresists in 4D printing.[126-128] There are different types of photoresists that are compatible with this kind of application. One way to design micro- and nanostructures by 3D laser lithography, is by stimuli-responsive hydrogels consisting of stimuli-responsive monomers, crosslinkers and a photoinitiator dissolved in water. Since most of these systems rely on swelling or shrinkage, the ratio monomer/crosslinker is critical. Stimuli-responsive monomers containing acrylates or acrylamides and functional groups, e.g., carboxylic acids are common. To ensure the integrity of the hydrogels structure, it is important to select a crosslinker that can provide support. Ideally, the crosslinker consists of monomers with a minimum of two polymerizable groups, such as *N,N'*-methylene bisacrylamide. Photoinitiators employed in these systems need to meet specific requirements, including a high two-photon cross-section, solubility in polar solvents and low cytotoxicity. These criteria can be satisfied by employing BAPO-Li as a photoinitiator (**Table 2d**).[126] Furthermore, advancements in this process have been achieved by combining alkoxyamine chemistry with TPA, resulting in the ability to print 'living' 3D microstructures.[127] By including covalent adaptable

microstructures (CAMs), the 3D structure can be modified after printing by e.g., nitroxide mediated polymerization (CAM-NER). The photoresist consists of TEMPO-methacrylate as nitroxide-donor, styrene as monomer, PEGDA as crosslinker, DETC as photoinitiator and a high boiling point solvent like dimethylformamide (**Table 2e**).[127] Through optimal adjustment of the ratios of the individual components, printing living 3D microstructures becomes realizable. **Figure 9a-c** illustrates three different shapes and their impressive size growth after 2 and 4 h polymerization.

In addition to their application in 3D laser lithography, (meth)acrylate-based photoresists have been utilized in DLP to fabricate both 3D and 4D structures.[129-133] For instance, Wang and co-workers fabricated 3D structures that are capable of responding to humidity and temperature.[134] The photoresist formulation is illustrated in **Table 2f**. The resulting printed architectures exhibited bending and twisting deformations triggered by moisture and could revert to their original shapes by adjusting to environmental conditions. By immersing especially printed 2D slices into water, a range of complex 3D architectures, such as a triangular pyramid, windmill, octopus and hydroturbine shapes were successfully obtained (**Figure 9d-g**). 2D-3D morphological transformation was also reported by Wu *et al*.[135] The photoresist consisted of acrylic acid as the monomer, *N,N'*-methylene bisacrylamide as the crosslinker, Sudan I dye as the photoabsorber, and Irgacure-819 as the photoinitiator (**Table 2g**). In this instance, biomimetic structures, such as cabbage, flowers, leaves, and Bauhinia pods evolved from predesigned 2D printed structures when immersed in water (**Figure 9h-k**).
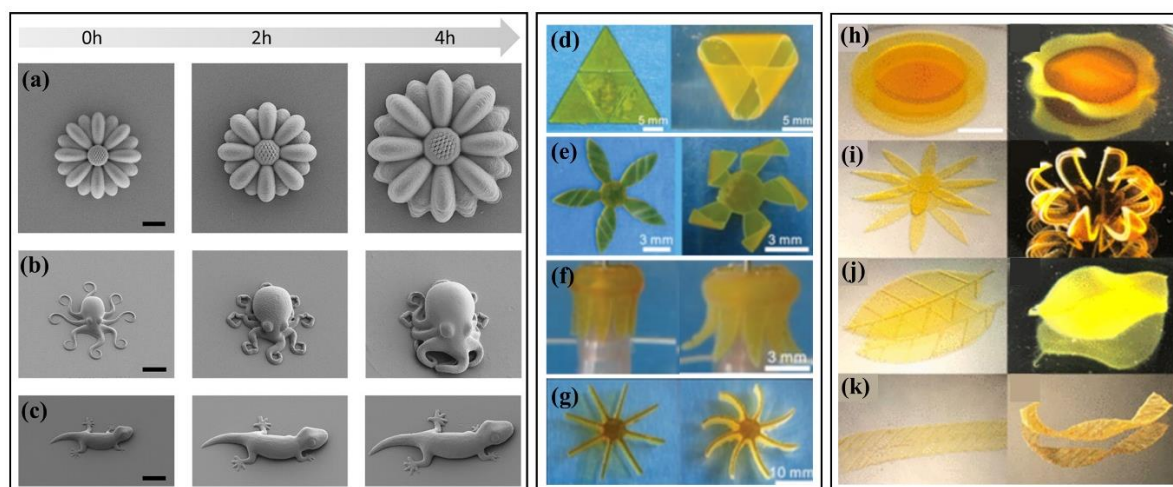
Figure 9. (a-c) SEM images of CAM microstructures after reaction times of 0, 2 and 4 h: (a) A CAM sunflower, (b) a CAM octopus and (c) a CAM gecko. Scale bars: 20 µm. Adapted with permission.[127] Copyright 2022, Wiley-VCH. (d-g) 2D-3D complex shape morphing when immersed in water. Adapted with permission.[134] Copyright 2019, Wiley-VCH. (h-k) Biomimetic structures evolved from predesigned 2D printed structures when immersed in water. Scale bar: 5 mm. Adapted with permission.[135] Copyright 2019, American Chemical Society.

4.2.2. Thiol-Ene-Based Photoresists

Photoinitiated thiol-ene radical reactions effectively are rapid light-triggered ligation reactions, resulting in a powerful approach for chemical synthesis and the fabrication of functional materials.[136] The reaction commences when a suitable photoinitiator generates a thiyl radical, which adds to the C=C double bond of the alkene forming an intermediate radical via a step-growth mechanism (**Figure 10a**). Subsequently, the intermediate radical abstracts a hydrogen from another thiol, generating a new thiyl radical thus repeating the cycle. However, when electron-deficient alkenes such as meth(acrylates) are incorporated into the thiol-ene reaction, the intermediate radical can also participate in a chain-growth mechanism (**Figure 10a**).[137] Consequently, the combination of both mechanisms leads to a complex network of thiol-ene, and homopolymerized meth(acrylate) segments.[138,139] One notable advantage of thiol-ene-based photoresists in comparison to their

meth(arylate)-based counterparts, is their relatively high gel point, i.e., the point at which a photoresist transitions from a liquid to gel-like state. As a result, shrinkage stress is reduced during the printing process, resulting in improved printing resolution.[136] In addition, thiol-ene-based photoresists are relatively insensitive to oxygen inhibition, eliminating the need to print in an inert atmosphere or employing high light intensities.[140] Commonly employed thiol monomers or their derivatives in 3D printing are trimethylolpropane tris(3-mercaptopropionate) (TMPMP),[141-143] pentaerythritol tetra(3-mercaptopropionate) (PETMP),[144-146] and tris[2-(3-mercaptopropionyloxy)ethyl] isocyanurate (TMI)[147,148] (**Figure 10b**).
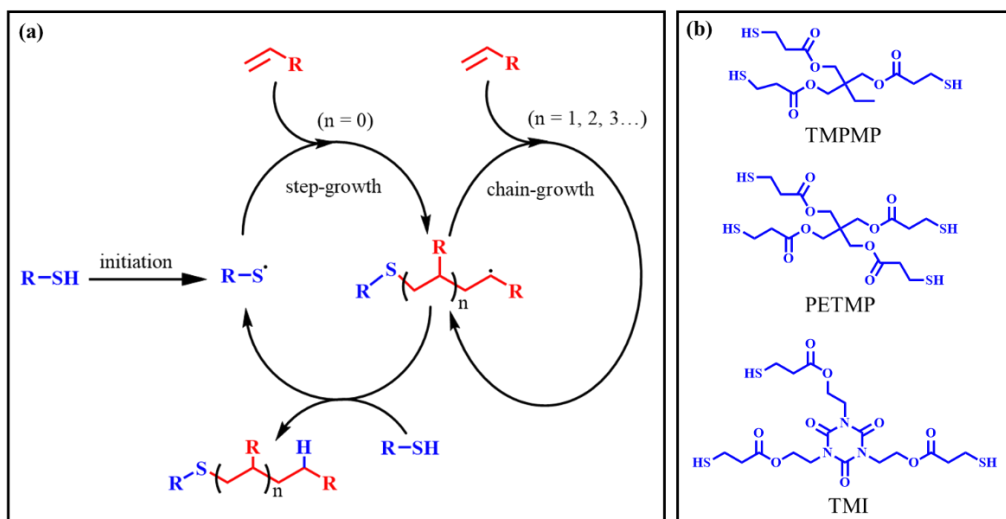
Figure 10. (a) The mechanism of a photoinitiated thiol-ene radical reaction. (b) Examples of thiol-based monomers commonly utilized in 3D printing (TMPMP; trimethylolpropane tris(3-mercaptopropionate), PETMP; pentaerythritol tetra(3-mercaptopropionate), TMI; tris[2-(3-mercaptopropionyloxy)ethyl] isocyanurate).

The pursuit of a photoresist formulation that allows the fabrication of 3D structures capable of being erased by visible light remains a significant challenge. Thus far, many photo-erasable inks require high-energy UV light, which is problematic for many applications, especially involving living cells. In addition, longer wavelengths inherently penetrate deeper into soft matter and are thus critically important for triggering post-printing properties from 3D-structures. The Barner-Kowollik group recently reported a breakthrough by exploiting the thiol-norbornene photo-click reaction for rapid

WILEY-VCH

DLW fabrication, along with the photodegradation of the resulting bimane ester moiety for visible light induced degradation.[149] Specifically, the bisfunctional norbornene reacts with the four-armed thiol crosslinker when irradiated with a 780 nm laser (**Table 2h**). Subsequently, the resulting network is irradiated with λ_{max} = 415-435 nm in the presence of a polar solvent to induce the photocleavage of the bimane ester linkage. Since no significant degradation was observed after 30 h irradiation, the authors incorporated an additional thiol crosslinker (PEG-SH) to reduce the crosslinking density of the network, and to facilitate water diffusion. Having established the optimal photoresist formulation, the authors combined their resist with a non-degradable commercial resist to print a multi-material boxing-ring structure (**Figure 11a).** Subsequently, the boxing-ring structure was immersed in water and subjected to visible-light irradiation (λ_{max} = 415 nm), whereby only the bridges of the boxing-ring structure were completely de-crosslinked after 32 h.

Gillner and co-workers successfully employed stereolithography to fabricate 3D structures.[150] In this study, the photoresist consisted of a three-arm thiol monomer and a bisfunctional acrylate crosslinker (**Table 2i**). Although the authors state the absence of a photoinitiator, we hypothesize that the utilization of a short laser wavelength (266 nm) during the printing process triggers *in situ* radical generation, thereby initiating a chain-growth mechanism. Thus, we have included this example in the current subsection. Nevertheless, load-bearing 3D scaffolds were fabricated via stereolithography by exploiting thiol-ene photo-click chemistry (**Figure 11b-e**). Thus, highlighting that photoresist consisting of thiol- and ene-monomers provides promising opportunities for future 3D printing applications.
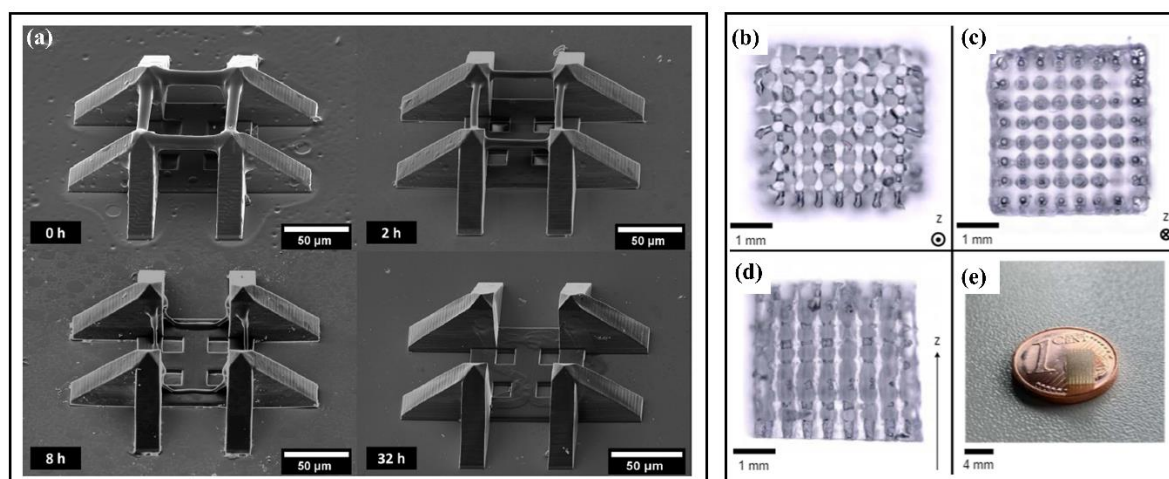
Figure 11. (a) SEM images of multi-material boxing ring structures, whereby only the bridges are erased when immersed in water and subjected to visible light irradiation for 32 h. Adapted with permission.[149] Copyright 2022, Wiley-VCH. (b-d) Microscopy images of 3D printed scaffolds from different perspectives, and (e) 3D scaffold on a one-cent coin. Adapted with permission.[150] Copyright 2021, Walter de Gruyter GmbH.

5. Future Direction of Photoresist Design

5.1 Action Plots for λ-Orthogonal Multi-Material Photoresists

Multi-material printing has emerged as an attractive potential avenue to fabricate advanced materials with disparate chemical and mechanical properties. These materials are inspired by natural systems, whereby hierarchical architectures play a significant role in enhancing their mechanical properties.[151,152] The ability to transfer these properties into the critical realm of 3D printing, could, for example, allow for fabricating structures with adaptive and self-healing properties. Nevertheless, bestowing multiple properties upon a single 3D structure is deemed a critical challenge. For the most part, this has been achieved by sequentially assembling the printed structure from separate photoresists, which can be extremely challenging and time-consuming.[103,104,122,149,153,154] A more elegant approach toward fabricating advanced materials is to use a single λ-orthogonal multi-material photoresist (**Figure 12a**).[155] The ability to print material A with λ_1 and material B with λ_2 – in any order

– would be considered a major breakthrough.[156] However, it is common that the absorption profiles of different chromophores partially overlap since most visible-light active species also show absorbance in the UV region. Consequently, it is only possible to trigger the photoreaction in a certain sequence, i.e., starting with irradiation at longer wavelengths, followed by irradiation at shorter wavelengths. One approach to overcome this challenge is to further separate the absorption bands of the employed chromophores, thereby reducing their spectral overlap. For example, the group of Read de Alaniz was able to sufficiently separate the absorption bands of various aniline-based donor-acceptor Stenhouse adducts (DASA).[157] Similarly, Feringa and co-workers combined a Stenhouse adduct with azobenzene.[33] In contrast to the aniline-based DASAs, the absorption bands of the azobenzene-based DASAs do not overlap at short wavelengths thus true λ-orthogonality was achieved.

Alternatively, true λ-orthogonality can be established by employing photochemical action plots. Whereas absorption spectra have long been utilized to identify the optimal irradiation wavelength for photoreactivity, they have recently been demonstrated to be unreliable in predicting the actual wavelength-dependent reactivity of a photoreactive chromophore. Over the last years, the Barner-Kowollik research team has shown – through the utilization of photochemical action plots – that the wavelength-dependent reactivity maximum frequently exhibits a red-shift compared to the absorption maximum. Essentially, irradiating a chromophore at its maximum wavelength of absorption will, in most instances, not yield the highest efficiency when it comes to conducting a photochemical reaction. It thus becomes imperative to explore the conversion of a photochemical process across monochromatic wavelengths in order to identify the most efficient irradiation conditions. As a result, an action plot is obtained by mapping the reaction conversion as a function of wavelength, offering more comprehensive insights into photoreactivity compared to absorption spectra. Indeed, such precise photochemical action plots have been vital toward developing λ-orthogonal multi-material photoresists. For example, the Barner-Kowollik team identified two photoreactive species, i.e., an *o*-methyl benzaldehyde (*o*-MBA) and a styrylpyrene (StyP), which according to their absorption profiles, cannot be activated independently from each other (**Figure 12b**).[158,159] However, an action plot analysis revealed a UV region where the StyP dimerization is sufficiently suppressed, yet the photoreactivity of the *o*-MBA is near its maximum efficiency (**Figure**

12c).[62] After identifying this orthogonal window based on photoreactivity, the two species were implemented into a λ-orthogonal multi-material photoresist to fabricate spatially resolved materials (**Figure 12d**).
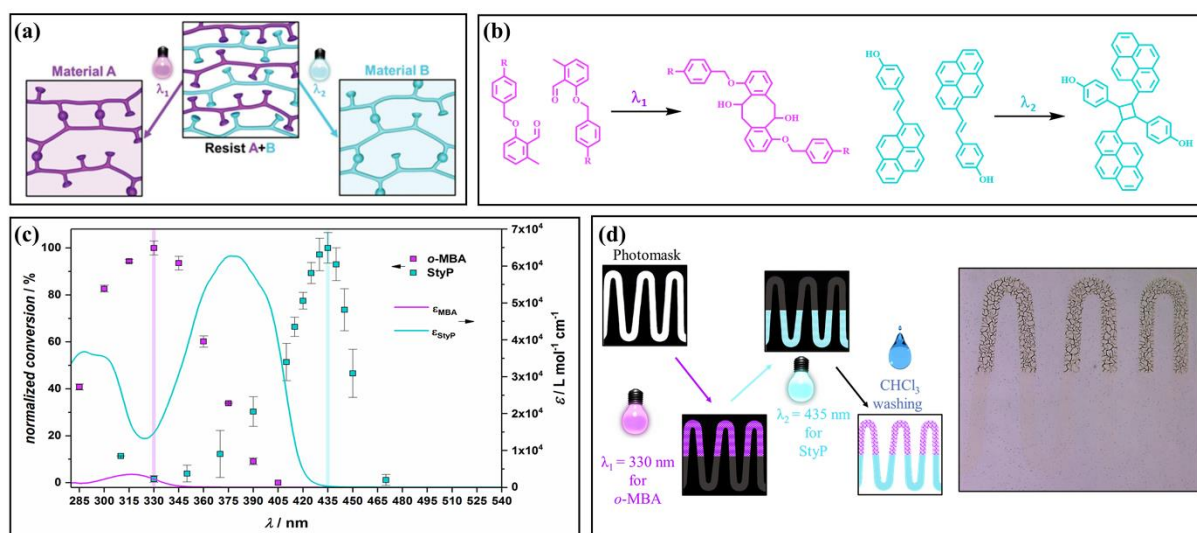
Figure 12. (a) Concept of the λ-orthogonal multi-material photoresist, whereby material A is printed with λ_1 and material B is printed with λ_2. (b) A Photoresist consisting of o-MBA (left) and StyP (right), which are capable of undergoing photodimerization. (c) Action plot (squares) and extinction coefficients (lines) of o-MBA and StyP revealing an orthogonal window based on photoreactivity. (d) A developed photoresist layer with a clear contrast between o-MBA and StyP after irradiating with 330 and 435 nm, respectively. Adapted with permission.[62] Copyright 2019, Wiley-VCH.

6. Conclusions and Outlook

Light-driven 3D printing techniques such as DLW, SLA and DLP have revolutionized the way objects are designed and manufactured. By exploiting the synergy between photochemistry and photoresists, these techniques have allowed for fabricating 3D structures with remarkable complexity. Combining these two disciplines continues to unlock exciting possibilities, enabling the creation of increasingly intricate and functional 3D structures that push the boundaries of what was once considered science fiction. For example, the possibility of erasing a 3D printed structure using visible light was once deemed unattainable. However, significant progress in photoresist technology has not only enabled

WILEY-VCH

degradation under visible light but even surpassed expectations by allowing degradation in the absence of light. These achievements have re-ignited exploration and renewed focus toward erasing structures exclusively with green or longer wavelengths. In addition, wavelength-orthogonal printing represents a significant advancement in light-driven 3D printing, enabling the fabrication of complex and functional structures. Undoubtedly, the capability to utilize disparate colors of light to print different materials from a single photoresist cartridge holds tremendous potential for streamlining the fabrication of multi-functional structures. Previously not considered for photochemical bond forming and cleavage reactions, the emergence of photochemical action plots and their incorporation into photoresist design has now brought this concept closer to reality. Owing to the rapid advances in photochemical photoresist design, we are highly optimistic that other 'so called' unattainable functions are now within our reach, such as the ability for a photoresist to autonomously repair itself when damaged and/or be printed by wavelengths surpassing 1000 nm. In addition, we envision a not-too-far-distant future where the functions of a photoresist are no longer constrained by technology but instead limited only by our imagination: precision photochemistry is the key to unlocking these possibilities.

References

[1]   N. Brown, P. Ertl, R. Lewis, T. Luksch, D. Reker, N. Schneider, *J. Comput. Aided Mol. Des.* **2020**, *34*, 709.

[2]   V. Kaul, S. Enslin, S. A. Gross, *Gastrointest. Endosc.* **2020**, *92*, 807.

[3]   C. Zhang, Y. Lu, *J. Ind. Inf. Integr.* **2021**, *23*, 100224.

[4]   Y. Wang, P. Zheng, T. Peng, H. Yang, J. Zou, *Sci. China. Technol. Sci.* **2020**, *63*, 1600.

[5]   G. Mattera, L. Nele, D. Paolella, *J. Intell. Manuf.* **2023**.

[6]   B. Heiden, V. Alieksieiev, M. Volk, B. Tonino-Heiden, *Procedia. Comput. Sci.* **2021**, *186,* 387-394.

[7]   Z. Jin, Z. Zhang, G. X. Gu, *Adv. Intell. Syst.* **2020**, *2*, 1900130.

[8]   D. Verma, Y. Dong, M. Sharma, A. K. Chaudhary, *Mater. Manuf.* **2022**, *37*, 518.

[9]   N. M. Bojanowski, A. Vranic, V. Hahn, P. Rietz, T. Messer, J. Brückel, C. Barner‐Kowollik, E. Blasco, S. Bräse, M. Wegener, *Adv. Funct. Mater.* **2022**, 2212482.

[10]   V. Ferraro, C. R. Adam, A. Vranic, S. Bräse, *Adv. Funct. Mater.* **2023**, 2302157.

[11]   I. M. Irshadeen, S. L. Walden, M. Wegener, V. X. Truong, H. Frisch, J. P. Blinco, C. Barner-Kowollik, *J. Am. Chem. Soc.* **2021**, *143*, 21113.

[12]   S. L. Walden, H. Frisch, B. V. Unterreiner, A.-N. Unterreiner, C. Barner-Kowollik, *J. Chem. Educ.* **2020**, *97*, 543.

[13]   I. M. Irshadeen, K. De Bruycker, A. S. Micallef, S. L. Walden, H. Frisch, C. Barner-Kowollik, *Polym. Chem.* **2021**, *12*, 493.

[14]   P. W. Kamm, J. P. Blinco, A.-N. Unterreiner, C. Barner-Kowollik, *ChemComm.* **2021**, *57*, 3991.

WILEY-VCH

[15]   D. E. Marschner, P. W. Kamm, H. Frisch, A.-N. Unterreiner, C. Barner-Kowollik, *ChemComm.* **2020**, *56*, 1443.

[16]   K. Kalayci, H. Frisch, V. X. Truong, C. Barner-Kowollik, *Nat. Commun.* **2020**, *11*, 4193.

[17]   J. L. Pelloth, P. A. Tran, A. Walther, A. S. Goldmann, H. Frisch, V. X. Truong, C. Barner-Kowollik, *Adv. Mater.* **2021**, *33*, 2102184.

[18]   C. Ma, T. Han, S. Efstathiou, A. Marathianos, H. A. Houck, D. M. Haddleton, *Macromolecules.* **2022**, *55*, 9908.

[19]   J. A. Reeves, N. De Alwis Watuthanthrige, C. Boyer, D. Konkolewicz, *ChemPhotoChem.* **2019**, *3*, 1171.

[20]   J. Hobich, E. Blasco, M. Wegener, H. Mutlu, C. Barner‐Kowollik, *Macromol. Chem. Phys.* **2023**, *224*, 2200318.

[21]   S. L. Walden, L. L. Rodrigues, J. Alves, J. P. Blinco, V. X. Truong, C. Barner-Kowollik, *Nat. Commun.* **2022**, *13*, 2943.

[22]   D. E. Fast, A. Lauer, J. P. Menzel, A.-M. Kelterer, G. Gescheidt, C. Barner-Kowollik, *Macromolecules.* **2017**, *50*, 1815.

[23]   A. Selimis, V. Mironov, M. Farsari, *Microelectron. Eng.* **2015**, *132*, 83.

[24]   D. Gräfe, S. L. Walden, J. Blinco, M. Wegener, E. Blasco, C. Barner-Kowollik, *Angew. Chem. Int. Ed.* **2020**, *59*, 6330.

[25]   F. P. W. Melchels, J. Feijen, D. W. Grijpma, *Biomaterials.* **2010**, *31*, 6121.

[26]   R. M. Hensleigh, H. Cui, J. S. Oakdale, J. C. Ye, P. G. Campbell, E. B. Duoss, C. M. Spadaccini, X. Zheng, M. A. Worsley, *Mater. Horiz.* **2018**, *5*, 1035.

[27]   X. Zheng, H. Lee, T. H. Weisgraber, M. Shusteff, J. DeOtte, E. B. Duoss, J. D. Kuntz, M. M. Biener, Q. Ge, J. A. Jackson, S. O. Kucheyev, N. X. Fang, C. M. Spadaccini, *AAAS.* **2014**, *344*, 1373.

[28]   M. M. Prabhakar, A. Saravanan, A. H. Lenin, K. Mayandi, P. S. Ramalingam, *Mater. Today: Proc.* **2021**, *45*, 6108.

[29]   Y. Bao, *Macromol. Rapid Commun.* **2022**, *43*, 2200202.

[30]   E. M. Maines, M. K. Porwal, C. J. Ellison, T. M. Reineke, *Green Chem.* **2021**, *23*, 6863.

WILEY-VCH

[31]   S. Aubert, M. Bezagu, A. C. Spivey, S. Arseniyadis, *Nat. Rev. Chem.* **2019**, *3*, 706.

[32]   H. Frisch, D. E. Marschner, A. S. Goldmann, C. Barner‐Kowollik, *Angew. Chem. Int. Ed.* **2018**, *57*, 2036.

[33]   M. M. Lerch, M. J. Hansen, W. A. Velema, W. Szymanski, B. L. Feringa, *Nat. Commun.* **2016**, *7*, 12054.

[34]   W. Szymański, J. M. Beierle, H. A. V. Kistemaker, W. A. Velema, B. L. Feringa, *Chem. Rev.* **2013**, *113*, 6114.

[35]   G. Ciamician, *Science.* **1912**, *36*, 385.

[36]   D. H. R. Barton, P. de Mayo, M. Shafiq, *J. Chem. Soc.* **1958**, 140-145.

[37]   M. J. Hansen, W. A. Velema, M. M. Lerch, W. Szymanski, B. L. Feringa, *Chem. Soc. Rev.* **2015**, *44*, 3358.

[38]   G. Kaur, P. Johnston, K. Saito, *Polym. Chem.* **2014**, *5*, 2171.

[39]   A. Balena, M. Bianco, F. Pisanello, M. De Vittorio, *Adv. Funct. Mater.* 2211773.

[40]   B. Kwon, J. H. Kim, *J. Nanosci.* **2016**, *2016*.

[41]   S. Heiskanen, Z. Geng, J. Mastomäki, I. J. Maasilta, *Adv. Eng. Mater.* **2020**, *22*, 1901290.

[42]   Y. Ozaki, S. Ito, T. Nakamura, M. Nakagawa, *Jpn. J. Appl. Phys.* **2019**, *58*, SDDJ04.

[43]   J. Stowers, D. A. Keszler, *Microelectron. Eng.* **2009**, *86*, 730.

[44]   M. Chambonneau, X. Wang, X. Yu, Q. Li, D. Chaudanson, S. Lei, D. Grojo, *Opt. Lett.* **2019**, *44*, 1619.

[45]   S. Heiskanen, Z. Geng, J. Mastomäki, I. J. Maasilta, *Adv. Eng. Mater.* **2020**, *22*, 1901290.

[46]   T. Frenzel, M. Kadic, M. Wegener, *AAAS.* **2017**, *358*, 1072.

[47]   M. Kadic, G. W. Milton, M. van Hecke, M. Wegener, *Nat. Rev. Phys.* **2019**, *1*, 198.

[48]   V. Hahn, T. Messer, N. M. Bojanowski, E. R. Curticean, I. Wacker, R. R. Schröder, E. Blasco, M. Wegener, *Nat. Photonics.* **2021**, *15*, 932.

[49]   T. D. Ngo, A. Kashani, G. Imbalzano, K. T. Q. Nguyen, D. Hui, *Compos. B: Eng.* **2018**, *143*, 172.

[50]   A. Aimar, A. Palermo, B. Innocenti, *J. Healthc. Eng.* **2019**, *2019*, 5340616.

WILEY-VCH

[51]   M. E. Prendergast, J. A. Burdick, *Adv. Mater.* **2020**, *32*, 1902516.

[52]   M. Mukhtarkhanov, A. Perveen, D. Talamona, *Micromachines.* **2020**, *11*, 946.

[53]   V. V. Krongauz, A. D. Trifunac, *Processes in Photoreactive Polymers.* **1995**, *1*.

[54]   V. Fouque, *Librairie des auteurs et de l'Académie des bibliophiles*, **1867**.

[55]   N. Niépce, *Pavillon de la photographie du Parc naturel régional de Brotonne*, **1973**, *Vol 1*.

[56]   X. Wang, X. H. Qin, C. Hu, A. Terzopoulou, X. Z. Chen, T. Y. Huang, K. Maniura‐Weber, S. Pané, B. J. Nelson, *Adv. Funct. Mater.* **2018**, *28*, 1804107.

[57]   M. Hippler, E. Blasco, J. Qu, M. Tanaka, C. Barner-Kowollik, M. Wegener, M. Bastmeyer, *Nat. Commun.* **2019**, *10*, 232.

[58]   Y. Tao, C. Lu, C. Deng, J. Long, Y. Ren, Z. Dai, Z. Tong, X. Wang, S. Meng, W. Zhang, Y. Xu, L. Zhou, *Micromachines.* **2021**, *13*, 32.

[59]   M. del Pozo, C. Delaney, M. Pilz da Cunha, M. G. Debije, L. Florea, A. P. H. J. Schenning, *Small. Struct.* **2022**, *3*, 2100158.

[60]   Y.-W. Lee, H. Ceylan, I. C. Yasa, U. Kilic, M. Sitti, *ACS Appl Mater Interfaces* **2021**, *13*, 12759.

[61]   T. Ergin, N. Stenger, P. Brenner, J. B. Pendry, M. Wegener, *AAAS.* **2010**, *328*, 337.

[62]   S. Bialas, L. Michalek, D. E. Marschner, T. Krappitz, M. Wegener, J. Blinco, E. Blasco, H. Frisch, C. Barner‐Kowollik, *Adv. Mater.* **2019**, *31*, e1807288.

[63]   J. Fischer, M. Wegener, *Laser Photonics Rev.* **2013**, *7*, 22.

[64]   K.-S. Lee, R. H. Kim, D.-Y. Yang, S. H. Park, *Prog. Polym. Sci.* **2008**, *33*, 631.

[65]   B. Richter, V. Hahn, S. Bertels, T. K. Claus, M. Wegener, G. Delaittre, C. Barner-Kowollik, M. Bastmeyer, *Adv. Mater.* **2017**, *29*, 1604342.

[66]   A. Koroleva, A. Deiwick, A. Nguyen, S. Schlie-Wolter, R. Narayan, P. Timashev, V. Popov, V. Bagratashvili, B. Chichkov, *PLoS One.* **2015**, *10*, e0118164.

[67]   M. Straub, M. Gu, *Opt. Lett.* **2002**, *27*, 1824.

[68]   C. Delaney, J. Qian, X. Zhang, R. Potyrailo, A. L. Bradley, L. Florea, *J. Mater. Chem. C.* **2021**, *9*, 11674.

WILEY-VCH

[69]   S. D. Gittard, P. R. Miller, R. D. Boehm, A. Ovsianikov, B. N. Chichkov, J. Heiser, J. Gordon, N. A. Monteiro-Riviere, R. J. Narayan, *Faraday Discuss.* **2011**, *149*, 171.

[70]   W. Hull Charles, *US Patent US 4575330 A*, 1986.

[71]   G. Zhu, H. A. Houck, C. A. Spiegel, C. Selhuber-Unkel, Y. Hou, E. Blasco, *Adv. Funct. Mater.* **2023**, 2300456.

[72]   X. Ma, X. Qu, W. Zhu, Y.-S. Li, S. Yuan, H. Zhang, J. Liu, P. Wang, C. S. E. Lai, F. Zanella, *PNAS.* **2016**, *113*, 2206.

[73]   L. Horváth, Y. Umehara, C. Jud, F. Blank, A. Petri-Fink, B. Rothen-Rutishauser, *Sci. Rep.* **2015**, *5*, 7974.

[74]   J. Liu, J. He, J. Liu, X. Ma, Q. Chen, N. Lawrence, W. Zhu, Y. Xu, S. Chen, *Bioprinting.* **2019**, *13*, e00040.

[75]   *Nat. Biotechnol.* **2015**, *33*, 1014.

[76]   J. Tao, X. Xu, S. Wang, T. Kang, C. Guo, X. Liu, H. Cheng, Y. Liu, X. Jiang, J. Mao, *ACS Macro Lett.* **2019**, *8*, 563.

[77]   J. R. Tumbleston, D. Shirvanyants, N. Ermoshkin, R. Janusziewicz, A. R. Johnson, D. Kelly, K. Chen, R. Pinschmidt, J. P. Rolland, A. Ermoshkin, E. T. Samulski, J. M. DeSimone, *AAAS.* **2015**, *347*, 1349.

[78]   N. J. Turro, P. D. Bartlett, *J. Org. Chem.* **1965**, *30*, 1849.

[79]   T. Fedynyshyn, R. Goodman, A. Cabral, C. Tarrio, T. Lucatorto, *Proc. SPIE*. **2010**, *Vol. 7639*.

[80]   P. Mueller, M. Thiel, M. Wegener, *Opt. Lett.* **2014**, *39*, 6847.

[81]   A. Wickberg, C. Kieninger, C. Sürgers, S. Schlabach, X. Mu, C. Koos, M. Wegener, *Adv. Opt. Mater.* **2016**, *4*, 1203.

[82]   U. T. Sanli, T. Messer, M. Weigand, L. Lötgering, G. Schütz, M. Wegener, C. Kern, K. Keskinbora, *Adv. Mater. Technol.* **2022**, *7*, 2101695.

[83]   R. B. Woodward, R. Hoffmann, *J. Am. Chem. Soc.* **1965**, *87*, 395.

[84]   J. Bai, Z. Shi, X. Ma, J. Yin, X. Jiang, *Macromol. Rapid Commun.* **2022**, *43*, 2200055.

[85]   K. Kalayci, H. Frisch, C. Barner-Kowollik, V. X. Truong, *Adv. Funct. Mater.* **2020**, *30*, 1908171.

[86]   G. Feng, M. Gao, L. Wang, J. Chen, M. Hou, Q. Wan, Y. Lin, G. Xu, X. Qi, S. Chen, *Nat. Commun.* **2022**, *13*, 2652.

[87]   M. Sicignano, R. I. Rodríguez, J. Alemán, *Eur. J. Org. Chem.* **2021**, *2021*, 3303.

[88]   D. Sarkar, N. Bera, S. Ghosh, *Eur. J. Org. Chem.* **2020**, *2020*, 1310.

[89]   V. X. Truong, C. Barner-Kowollik, *Aust. J. Chem.* **2022**, *4*, 291.

[90]   M. V. Tsurkan, C. Jungnickel, M. Schlierf, C. Werner, *J. Am. Chem. Soc.* **2017**, *139*, 10184.

[91]   B. Tarek Benkhaled, K. Belkhir, T. Brossier, C. Chatard, A. Graillot, B. Lonetti, A.-F. Mingotaud, S. Catrouillet, S. Blanquer, V. Lapinte, *Eur. Polym. J.* **2022**, *179*, 111570.

[92]   Y. Chujo, K. Sada, T. Saegusa, *Macromolecules.* **1990**, *23*, 2693.

[93]   J. Ling, M.-z. Rong, M.-q. Zhang, *Chin. J. Polym. Sci.* **2014**, *32*, 1286.

[94]   K. Saigo, *Prog. Polym. Sci.* **1992**, *17*, 35.

[95]   W. G. Kim, *J. Appl. Polym. Sci.* **2008**, *107*, 3615.

[96]   S. R. Trenor, T. E. Long, B. J. Love, *Macromol. Chem. Phys.* **2004**, *205*, 715.

[97]   Y. Inaki, H. Hiratsuka, *J. Photopolym. Sci. Technol.* **2000**, *13*, 739.

[98]   P. Froimowicz, H. Frey, K. Landfester, *Macromol. Rapid Commun.* **2011**, *32*, 468.

[99]   M. Gernhardt, E. Blasco, M. Hippler, J. Blinco, M. Bastmeyer, M. Wegener, H. Frisch, C. Barner‐Kowollik, *Adv. Mater.* **2019**, *31*, 1901269.

[100]   R. Batchelor, T. Messer, M. Hippler, M. Wegener, C. Barner-Kowollik, E. Blasco, *Adv. Mater.* **2019**, *31*, 1904085.

[101]   B. J. Adzima, C. J. Kloxin, C. A. DeForest, K. S. Anseth, C. N. Bowman, *Macromol. Rapid Commun.* **2012**, *33*, 2092.

[102]   M. W. Tibbitt, A. M. Kloxin, K. U. Dyamenahalli, K. S. Anseth, *Soft Matter.* **2010**, *6*, 5100.

[103]   M. M. Zieger, P. Mueller, A. S. Quick, M. Wegener, C. Barner‐Kowollik, *Angew. Chem. Int. Ed.* **2017**, *56*, 5625.

[104]   S. C. Gauci, M. Gernhardt, H. Frisch, H. A. Houck, J. P. Blinco, E. Blasco, B. T. Tuten, C. Barner‐Kowollik, *Adv. Funct. Mater.* **2022**, 2206303.

WILEY-VCH

[105] S. C. Gauci, K. Ehrmann, M. Gernhardt, B. Tuten, E. Blasco, H. Frisch, V. Jayalatharachchi, J. P. Blinco, H. A. Houck, C. Barner-Kowollik, *Adv. Mater.* **2023**, *35,* e2300151.

[106] H. A. Houck, P. Müller, M. Wegener, C. Barner‐Kowollik, F. E. Du Prez, E. Blasco, *Adv. Mater.* **2020**, *32*, 2003060.

[107] J. C. Scaiano, L. J. Johnston, W. G. McGimpsey, D. Weir, *Acc. Chem. Res.* **1988**, *21*, 22.

[108] J. C. Scaiano, E. A. Lissi, M. V. Encina, *Rev. Chem Intermed.* **1978**, *2*, 139.

[109] J. Zhou, X. Allonas, A. Ibrahim, X. Liu, *Prog. Polym. Sci.* **2019**, *99*, 101165.

[110] A. Bagheri, J. Jin, *ACS Appl. Polym. Mater.* **2019**, *1*, 593.

[111] T. Wloka, M. Gottschaldt, U. S. Schubert, *Chem. Eur. J.* **2022**, *28*, e202104191.

[112] A.-V. Do, K. S. Worthington, B. A. Tucker, A. K. Salem, *Int. J. Pharm.* **2018**, *552*, 217.

[113] B. Huang, Y. Zhou, L. Wei, R. Hu, X. Zhang, P. Coates, F. Sefat, W. Zhang, C. Lu, *Ind. Eng. Chem. Res.* **2022**, *61*, 13052.

[114] H. Kadry, S. Wadnap, C. Xu, F. Ahsan, *Eur. J. Pharm. Sci.* **2019**, *135*, 60.

[115] A. Barkane, O. Platnieks, M. Jurinovs, S. Gaidukovs, *Polym. Degrad. Stab.* **2020**, *181*, 109347.

[116] W. Shan, Y. Chen, M. Hu, S. Qin, P. Liu, *Mater. Res. Express.* **2020**, *7*, 105305.

[117] X. Zhang, Y. Xu, L. Li, B. Yan, J. Bao, A. Zhang, *J. Appl. Polym. Sci.* **2019**, *136*, 47487.

[118] H. Hwangbo, S.-J. Jeon, *Korean J. Chem. Eng.* **2022**, *39*, 451.

[119] F. Mayer, D. Ryklin, I. Wacker, R. Curticean, M. Čalkovský, A. Niemeyer, Z. Dong, P. A. Levkin, D. Gerthsen, R. R. Schröder, M. Wegener, *Adv. Mater.* **2020**, *32*, 2002044.

[120] D. Gräfe, A. Wickberg, M. M. Zieger, M. Wegener, E. Blasco, C. Barner-Kowollik, *Nat. Commun.* **2018**, *9*, 2788.

[121] M. Buback, A. Feldermann, C. Barner-Kowollik, I. Lacík, *Macromolecules.* **2001**, *34*, 5439.

[122] M. Carlotti, O. Tricinci, V. Mattoli, *Adv. Mater. Technol.* **2022**, *7*, 2101590.

[123] V. Hahn, N. M. Bojanowski, P. Rietz, F. Feist, M. Kozlowska, W. Wenzel, E. Blasco, S. Bräse, C. Barner-Kowollik, M. Wegener, *ACS Photonics.* **2023**, *10*, 24.

WILEY-VCH

[124] V. Hahn, P. Rietz, F. Hermann, P. Müller, C. Barner-Kowollik, T. Schlöder, W. Wenzel, E. Blasco, M. Wegener, *Nat. Photonics.* **2022**, *16*, 784.

[125] N. M. Bojanowski, A. Vranic, V. Hahn, P. Rietz, T. Messer, J. Brückel, C. Barner-Kowollik, E. Blasco, S. Bräse, M. Wegener, *Adv. Funct. Mater.* **2022**, 2212482.

[126] C. A. Spiegel, M. Hippler, A. Münchinger, M. Bastmeyer, C. Barner-Kowollik, M. Wegener, E. Blasco, *Adv. Funct. Mater.* **2020**, *30*, 1907615.

[127] Y. Jia, C. A. Spiegel, A. Welle, S. Heißler, E. Sedghamiz, M. Liu, W. Wenzel, M. Hackner, J. P. Spatz, M. Tsotsalas, E. Blasco, *Adv. Funct. Mater.* **2022**, 2207826.

[128] C. A. Spiegel, M. Hackner, V. P. Bothe, J. P. Spatz, E. Blasco, *Adv. Funct. Mater.* **2022**, *32*, 2110580.

[129] H. Ding, M. Dong, Q. Zheng, Z. L. Wu, *Mol. Sys. Des. Eng.* **2022**, *7*, 117.

[130] Z. Zhao, J. Wu, X. Mu, H. Chen, H. J. Qi, D. Fang, *Macromol. Rapid Commun.* **2017**, *38*, 1600625.

[131] H. Hong, Y. B. Seo, D. Y. Kim, J. S. Lee, Y. J. Lee, H. Lee, O. Ajiteru, M. T. Sultan, O. J. Lee, S. H. Kim, C. H. Park, *Biomaterials.* **2020**, *232*, 119679.

[132] K. Du, J. Basuki, V. Glattauer, C. Mesnard, A. T. Nguyen, D. L. J. Alexander, T. C. Hughes, *ACS Appl. Polym. Mater.* **2021**, *3*, 3049.

[133] Y. Li, Q. Mao, X. Li, J. Yin, Y. Wang, J. Fu, Y. Huang, *Addit. Manuf.* **2019**, *30*, 100889.

[134] Z. Ji, C. Yan, B. Yu, X. Zhang, M. Cai, X. Jia, X. Wang, F. Zhou, *Adv. Mater. Technol.* **2019**, *4*, 1800713.

[135] D. Wu, J. Song, Z. Zhai, M. Hua, C. Kim, I. Frenkel, H. Jiang, X. He, *ACS Appl. Mater. Interfaces.* **2019**, *11*, 47468.

[136] C. E. Hoyle, C. N. Bowman, *Angew. Chem. Int. Ed.* **2010**, *49*, 1540.

[137] M. Sahin, S. Ayalur-Karunakaran, J. Manhart, M. Wolfahrt, W. Kern, S. Schlögl, *Adv. Eng. Mater.* **2017**, *19*, 1600620.

[138] A. F. Senyurt, H. Wei, C. E. Hoyle, S. G. Piland, T. E. Gould, *Macromolecules.* **2007**, *40*, 4901.

[139] S. K. Reddy, K. S. Anseth, C. N. Bowman, *Polymer* **2005**, *46*, 4212.

[140] A. K. O'Brien, N. B. Cramer, C. N. Bowman, *J. Polym. Sci., Part A: Polym. Chem.* **2006**, *44*, 2007.

[141] A. Oesterreicher, J. Wiener, M. Roth, A. Moser, R. Gmeiner, M. Edler, G. Pinter, T. Griesser, *Polym. Chem.* **2016**, *7*, 5169.

[142] D. G. Sycks, T. Wu, H. S. Park, K. Gall, *J. Appl. Polym. Sci.* **2018**, *135*, 46259.

[143] L. Strohmeier, H. Frommwald, S. Schlögl, *RSC Adv.* **2020**, *10*, 23607.

[144] B. Ch. Kholkhoev, Z. A. Matveev, A. N. Nikishina, V. F. Burdukovskii, *Mendeleev Commun.* **2022**, *32*, 813.

[145] A. Hoffmann, H. Leonards, N. Tobies, L. Pongratz, K. Kreuels, F. Kreimendahl, C. Apel, M. Wehner, N. Nottrodt, *J. Tissue Eng.* **2017**, *8*, 2041731417744485.

[146] Y. Shi, G. Fang, Z. Cao, F. Shi, Q. Zhao, Z. Fang, T. Xie, *Chem. Eng. J.* **2021**, *426*, 131306.

[147] C. C. Cook, E. J. Fong, J. J. Schwartz, D. H. Porcincula, A. C. Kaczmarek, J. S. Oakdale, B. D. Moran, K. M. Champley, C. M. Rackson, A. Muralidharan, R. R. McLeod, M. Shusteff, *Adv. Mater.* **2020**, *32*, 2003376.

[148] R. Bongiovanni, A. Vitale, "High Resolution Manufacturing from 2D to 3D/4D Printing" **2022**, 17.

[149] M. Gernhardt, V. X. Truong, C. Barner‐Kowollik, *Adv. Mater.* **2022**, *34*, 2203474.

[150] K. Kreuels, D. Bosma, N. Nottrodt, A. Gillner, *Curr. Dir. Biomed. Eng.* **2021**, *7*, 847.

[151] A. R. Studart, *Chem. Soc. Rev.* **2016**, *45*, 359.

[152] N. D. Dolinski, Z. A. Page, E. B. Callaway, F. Eisenreich, R. V. Garcia, R. Chavez, D. P. Bothman, S. Hecht, F. W. Zok, C. J. Hawker, *Adv. Mater.* **2018**, *30*, 1800364.

[153] M. M. Zieger, P. Müller, E. Blasco, C. Petit, V. Hahn, L. Michalek, H. Mutlu, M. Wegener, C. Barner‐Kowollik, *Adv. Funct. Mater.* **2018**, *28*, 1801405.

[154] M. Gernhardt, H. Frisch, A. Welle, R. Jones, M. Wegener, E. Blasco, C. Barner-Kowollik, *J. Mater. Chem. C.* **2020**, *8*, 10993.

[155] E. Rossegger, J. Strasser, R. Höller, M. Fleisch, M. Berer, S. Schlögl, *Macromol. Rapid Commun.* **2023**, *44*, 2200586.

[156] C. Barner-Kowollik, M. Bastmeyer, E. Blasco, G. Delaittre, P. Müller, B. Richter, M. Wegener, *Angew. Chem. Int. Ed.* **2017**, *56*, 15828.

[157] J. R. Hemmer, S. O. Poelma, N. Treat, Z. A. Page, N. D. Dolinski, Y. J. Diaz, W. Tomlinson, K. D. Clark, J. P. Hooper, C. Hawker, J. Read de Alaniz, *J. Am. Chem. Soc.* **2016**, *138*, 13960.

[158] T. Krappitz, F. Feist, I. Lamparth, N. Moszner, H. John, J. P. Blinco, T. R. Dargaville, C. Barner-Kowollik, *Mater. Horiz.* **2019**, *6*, 81.

[159] H. Frisch, D. Kodura, F. R. Bloesser, L. Michalek, C. Barner‐Kowollik, *Macromol. Rapid Commun.* **2020**, *41*, e1900414.

WILEY-VCH

Table of Contents

Enabling precision control over photochemical modulation is essential for designing advanced photoresists with diverse functionalities. Herein, we evaluate recent advances in photoresist design for light-driven 3D printing. We classify the discussed photoresists into chemistries that function photoinitiator-free and those that require a photoinitiator to proceed, enabling a comprehensive understanding of their capabilities, limitations, and realistic possibilities for the near future.

Steven C. Gauci, Aleksandra Vranic, Eva Blasco, Stefan Bräse, Martin Wegener, Christopher Barner-Kowollik*

Photochemically Activated 3D Printing Inks: Current Status, Challenges, and Opportunities

WILEY-VCH
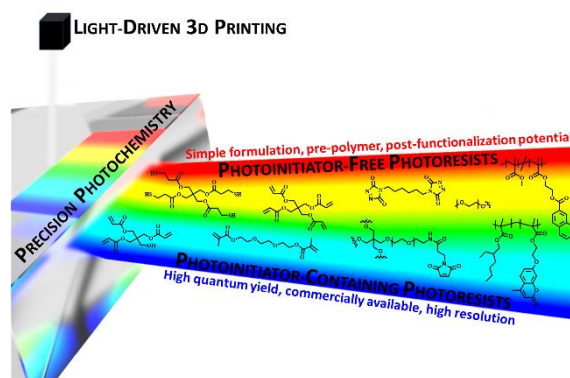
Author Biographies

Steven Gauci obtained a first-class BSc(Hons) degree in chemistry from Queensland University of Technology (QUT). Currently, he is pursuing his PhD at QUT under the supervision of Prof. Christopher Barner-Kowollik. His research interests mainly focus on the development of novel photoresists and functional materials for 3D laser lithography.

Aleksandra Vranic received her B.Sc. and M.Sc. degrees in Chemistry from the Karlsruhe Institute of Technology (Germany). She is currently working on her Ph.D., focusing on developing novel photoinitiators for 3D laser nanoprinting in Prof. Stefan Bräse's group at the Institute of Organic Chemistry, founded by the Karlsruhe School of Optics and Photonics (KSOP). She is also part of the 3DMM2O Cluster (Thrust A3).

Eva Blasco completed her Ph.D. studies at the University of Zaragoza (Spain). Thereafter, she obtained an Alexander von Humboldt Postdoctoral Fellowship to work in the groups of Prof. Barner-Kowollik and Prof. Wegener at the Karlsruhe Institute of Technology (KIT) in Germany and she continued as a group leader at the same institution. In October 2020, she was appointed junior professor at the University of Heidelberg (Germany) and in January 2023 she was promoted to full professor. She is a PI in the Excellence Cluster 3DMM2O and her research interests include the development of new functional materials for 3D/4D printing.

WILEY-VCH

Stefan Bräse studied chemistry in Göttingen, Bangor, and Marseille and received his Ph.D. in 1995 in Göttingen. After postdoctoral research at Uppsala and the Scripps Research, he began his independent research at the RWTH Aachen in 1997 and was promoted to professor in Bonn in 2001. Since 2003, he has been a professor at the Institute of Organic Chemistry, Karlsruhe Institute of Technology (KIT), and since 2012, also the Director of the Institute of Biological and Chemical Systems (ITG, now IBCS-FMS) at the KIT. His research interests include synthetic chemistry, molecular engineering of functional synthetic materials, and digitization in chemistry.

After completing his Diploma and PhD in physics at Johann Wolfgang Goethe-Universität Frankfurt (Germany) in 1986 and 1987, respectively, he spent two years as a postdoc at AT&T Bell Laboratories in Holmdel (U.S.A.). From 1990-1995 he was professor (C3) at Universität Dortmund (Germany), since 1995 he is professor (C4, later W3) at Institute of Applied Physics of Karlsruhe Institute of Technology (KIT). Since 2001 he has a joint appointment as department head at Institute of Nanotechnology (INT) of KIT. Since 2018 he is spokesperson of the Cluster of Excellence 3D Matter Made to Order.

A PhD graduate of Göttingen University, Germany, Christopher Barner-Kowollik joined the University of New South Wales in early 2000 rising to lead the Centre for Advanced Macromolecular Design as one of its directors. In 2008, he joined KIT, establishing a German Research Council funded Centre of Excellence. He moved to QUT in 2017, establishing QUT's Soft Matter Materials Laboratory. Over his 23-year career to date focussing on macromolecular photochemical processes, he supported highly collaborative large teams. He has authored over 760 peer-reviewed publications, which have been cited over 45,000 times. His multi-award-winning research explores precision orthogonal, synergistic and antagonistic photochemical reactions and their application in macromolecular systems.